Title:

Small RNA-mediated genomic silencing promotes telomere stability in the absence of telomerase

Authors:

Charlie Longtine[1,2,#], Stephen Frenk[1,2,#], and Shawn Ahmed[1,2*]

Affiliations:

[1]Department of Genetics, [2]Department of Biology, University of North Carolina, Chapel Hill, NC, USA

# Equal contributions
*Correspondence and Lead Contact: shawn@med.unc.edu

Short title: small RNAs promote telomere stability

Abstract

Telomerase deficiency in human somatic cells results in telomere erosion and senescence. Small RNAs that target telomeres have been observed in diverse organisms but their functions are not well characterized. We define an endogenous small RNA pathway in *Caenorhabditis elegans* that promotes heterochromatin formation at telomeres via Dicer, the perinuclear Argonaute protein WAGO-1 and the nuclear Argonaute protein HRDE-1. Loss of telomerase induces biogenesis of siRNAs that target the telomeric lncRNA TERRA, whereas loss of both telomerase and small RNA-mediated telomeric silencing induces TERRA expression, DNA damage, and an accelerated sterility phenotype. These phenotypes can be rescued by exogenous telomeric siRNAs or by loss of the DNA damage response protein EXO-1. Thus, endogenous siRNAs interact with TERRA to promote heterochromatin formation in a manner that is critical for the stability of naturally eroding telomeres. We propose that small RNA-mediated genome silencing could be broadly relevant to regulation of proliferative aging.

Introduction

Telomeres are repetitive nucleoprotein structures that protect the ends of linear eukaryotic chromosomes from degradation and recognition as double-stranded DNA breaks (Maciejowski and de Lange, 2017, Shay, 2016). In most human somatic cells, which are deficient for telomerase reverse transcriptase, telomeres erode over progressive cell divisions, eventually triggering replicative senescence (Holohan et al., 2014, Shay, 2016). Telomere shortening thus acts as a barrier to tumorigenesis, but may also contribute to organismal aging through impaired stem cell function, regeneration, and organ maintenance (Donate and Blasco, 2011, Shay, 2016). Regulating the rate of telomere erosion in telomerase-negative cells is therefore crucial to maintain this balance between tumor suppression and age-related tissue decline (Li et al., 2017, Maciejowski and de Lange, 2017). Tumor cells escape telomere-triggered senescence by stabilizing telomere length, either through reactivation of telomerase or through activation of the telomerase-independent recombination-mediated telomere

maintenance pathway termed Alternative Lengthening of Telomeres (ALT) (Pickett and Reddel, 2015).

Telomeres have features characteristic of heterochromatin in that they associate with the heterochromatin protein HP1 and contain transcriptionally repressive histone marks such as methylation of H3K9 and H4K20 (Benetti et al., 2007, McMurchy et al., 2017). Nonetheless, telomeres are transcribed into the G-rich long noncoding RNA (lncRNA) termed TERRA, a feature widely conserved among eukaryotes, and lower levels of the C-rich antisense lncRNA ARRET have also been reported (Azzalin et al., 2007). TERRA is transcribed from the subtelomere into the telomere by RNA polymerase II and is upregulated at shortened and damaged telomeres, where it may recruit telomerase and chromatin modifiers to promote telomere elongation (Azzalin and Lingner, 2015, Cusanelli et al., 2013). Telomere elongation represses expression of TERRA through increased methylation and HP1 binding (Arnoult et al., 2012). Notably, telomere shortening in mice with telomerase defects and overexpression of a negative regulator of telomere length have been associated with loss of heterochromatic marks at telomeres and subtelomeres (Benetti et al., 2007, Benetti et al., 2008).

Transcriptional silencing and heterochromatin deposition at repetitive segments of the genome such as the pericentromere (Holoch and Moazed, 2015, Reinhart and Bartel, 2002) require long non-coding RNA (lncRNA) transcripts that promote biogenesis of and interact with small RNAs that direct heterochromatin factors to target genomic loci. Endogenous sources of double-stranded RNA such as sense-antisense transcript hybrids can be processed into small RNAs that play roles in creating and maintaining siRNA-mediated heterochromatin, where paradoxically RNA expression is required for genomic silencing. Bidirectional transcription of telomeres has been linked to production of telomeric siRNAs that promote subtelomeric DNA methylation in *Arabidopsis* (Vrbsky et al., 2010). The presence of similar telomeric siRNAs has also been observed in *Tetrahymena*, mouse stem cells, and human cell lines (Cao et al., 2009, Rossiello et al., 2017), but their functional relevance at canonical telomeres is not well understood in any experimental system.

102

103 Germline transcription in *C. elegans* is regulated in part by a network of small RNA
104 pathways that promote silencing or expression of target loci in a sequence-specific
105 manner (Billi et al., 2014). Transcription of potentially harmful foreign genetic elements
106 including transposons and transgenes is repressed by 21 nucleotide PIWI-interacting
107 RNAs or piRNAs. These interact with PRG-1, a member of the PIWI clade of Argonaute
108 proteins that recognizes RNA targets of piRNAs based on sequence complimentarity
109 with up to 3 mismatches (Bagijn et al., 2012, Batista et al., 2008, Das et al., 2008). RNA
110 target recognition triggers the recruitment of RNA-dependent RNA polymerases
111 (RdRPs) that act in Mutator bodies, which are associated with perinuclear P granules, to
112 create *de novo* 22 nucleotide secondary siRNAs with a 5' guanine (22G RNAs) (Pak
113 and Fire, 2007). These 22G RNAs are loaded onto worm-specific Argonaute proteins
114 (WAGOs) such as the nuclear WAGO HRDE-1, which promotes heterochromatin
115 deposition at target loci (Ashe et al., 2012, Buckley et al., 2012). Germline transcription
116 is protected by a separate set of 22G RNAs that interact with the anti-silencing
117 Argonaute protein CSR-1 (Avgousti et al., 2012, Wedeles et al., 2013) . Aside from the
118 piRNA pathway, 22G activity can be triggered by primary siRNAs from other sources.
119 For example, DCR-1, the *C. elegans* homologue of the highly conserved RNAse class
120 III enzyme Dicer, can cleave endogenous and exogenous double stranded RNA
121 transcripts to create primary 26G RNAs, which bind a distinct set of Argonautes to
122 trigger target silencing through the 22G pathway described above (Bernstein et al.,
123 2001, Ketting et al., 2001, Knight and Bass, 2001).
124

125 Here we describe an endogenous siRNA pathway that represses TERRA via
126 heterochromatin formation and functions redundantly with telomerase to promote
127 telomere stability.
128

129 **Results**
130

131 **Loss of endogenous siRNAs or XNP-1/ATRX does not promote ALT**

High levels of TERRA and loss of the histone H3.3 chaperone subunits ATRX and DAXX commonly occur in human ALT cancers (Flynn et al., 2015, Lovejoy et al., 2012). The ATRX/DAXX complex mediates histone H3.3 incorporation at telomeres and interacts with methylated H3K9 and HP1 to promote heterochromatin formation (Wong et al., 2010), which has been proposed to repress ALT by protecting telomeres from replication stress and TERRA expression (Udugama et al., 2015). We have previously shown that 10-20% of *C. elegans* strains that are deficient for telomerase can be maintained indefinitely through the activation of ALT (Cheng et al., 2012). Because human ALT cancers are characterized by ATRX-mediated heterochromatin dysfunction, we reasoned that small RNA factors that promote heterochromatin silencing might regulate the establishment of ALT. We tested this hypothesis by passaging *trt-1* telomerase mutant strains that were deficient for biogenesis of either primary or secondary siRNAs by transferring 100s of worms per strain weekly, which reliably allows survival of 10-20% of strains via ALT (Cheng et al., 2012). Loss of either primary siRNAs (*trt-1; dcr-1)* or downstream secondary siRNAs (*trt-1; mut-7* and *trt-1; mut-14)* did not significantly alter the proportion of strains that survive via ALT (Figure 1A, Table S1). Similarly, loss of the histone H3.3 chaperone XNP-1/ATRX itself did not affect the establishment or maintenance of ALT (Table S1), indicating that loss of neither siRNA- nor XNP-1/ATRX-mediated heterochromatin formation is sufficient to promote ALT.

Small RNA and heterochromatin factors repress rapid sterility when telomerase is deficient

C. elegans strains mutant for telomerase reverse transcriptase, *trt-1,* become uniformly progressively sterile – analogous to crisis that is induced by telomere erosion, chromosome fusion and genome catastrophe in checkpoint-deficient telomerase-negative mammalian cells – when 6 worms are passaged weekly (Ahmed and Hodgkin, 2000), which eliminates survival via ALT (Cheng et al., 2012). Intriguingly, when passaged by transferring 6 L1 larvae per week, *trt-1* mutant lines lacking primary or secondary siRNA biogenesis factors became sterile significantly faster than *trt-1* single mutants (Figure 1B, Table S2). siRNA-deficient *trt-1* strains rapidly accumulated end-to-end chromosome fusions by generation F12, a characteristic of telomerase mutants

163 that have grown for more than 20 generations (Figure 1G). These strains also displayed
164 high levels of DNA damage by generation F6 that were not observed for *trt-1* single
165 mutant controls (Figure 1H). As oocyte karyotypes can only reliably detect the
166 presence of multiple chromosome fusions, we performed genetic crosses that would be
167 capable of detecting a single heterozygous end-to-end chromosome fusion (Ahmed and
168 Hodgkin, 2000). Chromosome fusions cause non-disjunction events during meiosis that
169 elicit dominant embryonic lethality or X0 male phenotypes in progeny of heterozygous
170 F1 animals. We crossed four independent *trt-1 dcr-1* F4 hermaphrodites and failed to
171 detect fused chromosomes that were present in generation F24 *trt-1* mutant controls (p
172 = 3.841e-05 for males and p = 3.61e-05 for dead embryos, Mann Whitney U test) (Table
173 S3). Together, these results suggest that loss of small RNAs and telomerase elicits
174 telomere damage but not telomere fusions in early generations, and that the rapid
175 sterility of these strains in later generations is promoted by critically shortened
176 telomeres that give rise to abundant end-to-end chromosome fusions. Small RNA
177 factors required to prevent this accelerated sterility included RDE-4, which binds
178 endogenous dsRNA and forms a complex with the Dicer nuclease DCR-1, and the
179 Argonaute RDE-1, which acts with the RNA-dependent RNA polymerase RRF-3 to
180 promote production of dsRNA-derived primary siRNAs (Gent et al., 2010, Steiner et al.,
181 2009, Tabara et al., 2002) (Figure 1B). The MUTATOR proteins MUT-7 and MUT-14,
182 which also were required to prevent rapid sterility in *trt-1* (Figure 1B), promote
183 amplification of 22G secondary siRNAs that act as downstream effector siRNAs by
184 promoting mRNA degradation in the cytoplasm or transcriptional silencing in the
185 nucleus (Billi et al., 2014, Ketting et al., 1999, Tijsterman et al., 2002).
186
187 Southern blotting suggested that *dcr-1* and *mut-14* single mutants do not have shorter
188 telomeres than wildtype or *trt-1* mutant strains (Figure S1), which implies that the
189 accelerated sterility of small RNA-deficient *trt-1* mutant strains is unlikely to be a
190 consequence of short telomeres that are inherited from gametes of small RNA-deficient
191 grandparents. We tested this premise using genetics, by crossing a *trt-1; dcr-1* double
192 mutant hermaphrodite with *dcr-1* mutant males, singling *trt-1 +/-; dcr-1 -/-* F1
193 hermaphrodites and isolating *trt-1; dcr-1* double mutant F2. This cross was repeated 15

194 times, to create a *trt-1; dcr-1* double mutant strain whose telomeres should be
195 exclusively derived from the *dcr-1* mutant background. The *trt-1; dcr-1* 15x strain
196 became sterile slightly more slowly than freshly created *trt-1; dcr-1* double mutants (p =
197 0.07) (Fig. 1H), indicating that shortened telomeres transmitted from the *dcr-1* mutant
198 cannot explain the rapid sterility of *trt-1; dcr-1* double mutants. Because none of the
199 small RNA single mutants tested became progressively sterile or accumulated
200 chromosome fusions (Figure 1G), we conclude that telomere maintenance is not
201 impaired in small RNA-deficient lines in the presence of telomerase. We analyzed the
202 dynamics of telomere erosion using terminal restriction fragment analysis, but did not
203 observe an obvious difference between *trt-1* and siRNA-deficient *trt-1* mutant strains
204 (Figure S2). Two other small RNA factors, RRF-2 and ERI-1, were not required to
205 prevent rapid onset of sterility, indicating that the endogenous siRNA pathway that
206 requires ERI-1 (Gent et al., 2010, Han et al., 2009) is dispensable for telomere
207 protection in the absence of telomerase (Figure 1B).
208
209 We hypothesized that small RNAs might repress rapid sterility by directing chromatin
210 factors to telomeres to promote deposition of heterochromatic marks. *C. elegans*
211 telomeres have previously been reported to be enriched for H3K9me2 and bound by the
212 HP1 homolog HPL-2, which promotes H3K9me2 deposition and heterochromatin
213 formation, but not by the other *C. elegans* HP1 homolog HPL-1, which interacts with
214 H3K9me3 (Canzio et al., 2014, McMurchy et al., 2017). We confirmed that H3K9me2
215 but not H3K9me3 was enriched at *C. elegans* telomeres using high throughput
216 sequencing data sets generated from chromatin immunoprecipitation (ChIP)
217 experiments performed by independent groups (McMurchy et al., 2017, Zeller et al.,
218 2016). Moreover, we observed small H3K9me2 domains that extended into the
219 subtelomere at all twelve *C. elegans* chromosome ends (Figure 3A-D). H3K4
220 methylation, which is associated with regions of active transcription, must be removed
221 by demethylases prior to deposition of repressive H3K9 methylation (Greer et al., 2010,
222 Li et al., 2008). Similar to primary and secondary siRNA-deficient *trt-1* strains, loss of
223 HPL-2 but not HPL-1, and loss of either of the two *C. elegans* H3K4 demethylases
224 RBR-2/KDM5 or SPR-5/LSD1, caused accelerated senescence in *trt-1* mutants (Figure

225 1C). Thus, H3K4 demethylation and H3K9me2 deposition prevent telomere instability in
226 the absence of telomerase.
227
228 The histone remodeling protein XNP-1/ATRX has previously been implicated in
229 telomeric heterochromatin formation and interacts with unmethylated H3K4 and
230 methylated H3K9 deposited on the histone variant H3.3 (Udugama et al., 2015). *trt-1*
231 *xnp-1* double mutants went sterile significantly faster than *trt-1* single mutants but not as
232 fast as small RNA deficient *trt-1; mut-7* double mutants (Figure 1D). This suggests that
233 XNP-1 may mediate some, but not all heterochromatin formation at telomeres, possibly
234 because siRNA-dependent methylation of histones other than H3.3, such as canonical
235 histone H3 or H4 can promote telomere stability. Additionally, because loss of both
236 XNP-1 and MUT-7 did not cause an additive effect on survival in *trt-1* mutant strains
237 (Figure 1D), these genes may function in the same pathway, which implies that siRNAs
238 direct the chromatin remodeler XNP-1 to telomeres to repress rapid sterility in the
239 absence of telomerase.
240
241 **Increased expression of TERRA in small RNA and chromatin deficient *trt-1* strains**
242 We hypothesized that DCR-1 and RDE-4 may interact with telomeric dsRNA produced
243 from bidirectional transcription of telomeres into TERRA and ARRET, to create primary
244 siRNAs that are then amplified into a secondary siRNA population that triggers small
245 RNA-dependent silencing of TERRA (Rossiello et al., 2017, Vrbsky et al., 2010). To
246 test whether small RNA and chromatin factors regulate telomeric transcription we
247 measured the abundance of TERRA by qRT-PCR at three chromosome ends using
248 primers within their H3K9me2-coated subtelomere domains (Figure 3A-D). Compared
249 to *trt-1* single mutant controls, TERRA was upregulated in early-generation *trt-1; rde-4*,
250 and *trt-1; mut-14* and *trt-1; spr-5* double mutants (Figure 2A). These high levels of
251 TERRA transcription were markedly induced in small RNA and heterochromatin
252 mutants that lacked telomerase, consistent with the hypothesis that TERRA
253 transcription is specifically induced at damaged or shortened telomeres (Porro et al.,
254 2014, Rossiello et al., 2017).
255

256 We next used RNA Fluorescence *In Situ* Hybridization (FISH) to confirm the effects on
257 TERRA expression and to examine its cell and tissue localization. In wildtype control
258 and *trt-1* mutant hermaphrodite and male worms, TERRA was expressed at low levels
259 in the soma as well as the pachytene region of the meiotic germline (Figures 2B-D, S3-
260 4), which corresponds to the location of several lncRNA-mediated germline silencing
261 processes (Taylor et al., 2015), including Meiotic Silencing of Sex Chromosomes in
262 mammals and *C. elegans* (Heard and Turner, 2011) and a transcriptional burst of
263 piRNAs in mammals that primes genomic silencing in germ cells prior to gametogenesis
264 (Gou et al., 2014). Compared to both wildtype control and *trt-1* or *dcr-1* single mutant
265 strains, *trt-1; dcr-1* double mutant strains had increased expression of TERRA in the
266 germline (Figures 2B-D, S3) and soma (Figures S3-4) by the F6 generation.
267 Endogenous siRNAs thus regulate telomeric transcription in both the soma and
268 germline during telomere attrition, likely through the production of siRNAs that directly
269 target the heterochromatin factors HPL-2, RBR-2 and SPR-5 to telomeres.
270
271 **Subtelomeric siRNAs are upregulated in telomerase mutants**
272 Telomeric siRNAs have been observed in protists, plants and mammals (Cao et al.,
273 2009, Vrbsky et al., 2010). We therefore interrogated 92 publicly available small RNA
274 sequencing libraries created from RNA isolated from various *C. elegans* strains and
275 found rare reads that mapped perfectly to the *C. elegans* telomere repeat $(TTAGGC)_n$,
276 occurring at a frequency of 1 per 10,000,000 reads. piRNAs with up to 3 mismatches
277 can target regions of the *C. elegans* genome for silencing (Bagijn *et al.*, 2012) , and we
278 found that telomeric siRNAs with up to 3 mismatches were substantially more abundant
279 than those with perfect telomere repeat sequence (1 per 100,000). Telomeric siRNAs
280 with zero to two mismatches were significantly more likely to be composed of the
281 telomeric G-strand sequence than would be expected by chance ($p < 2.2e-16$, binomial
282 test) (Figure 3E). The proportion of telomeric siRNAs with one or two mismatches
283 beginning with a G nucleotide was significantly greater than that for all mappable reads
284 ($p < 1e-15$, Fisher's exact test) and the median length for these RNAs was 22
285 nucleotides (Figure 3D, F), suggesting that telomeric siRNAs mapping imperfectly to
286 telomeres are enriched for 22G RNA species. This is consistent with the model that

287 primary siRNAs recruit RNA-dependent RNA polymerases to target RNAs in order to
288 create secondary effector siRNA populations de novo that are highly enriched for 22G
289 RNAs (Gu et al., 2009). We compared levels of telomeric siRNAs from wild-type with
290 those of small RNA mutants that promote telomere stability in the absence of
291 telomerase, such as *dcr-1*, *rde-4*, *mut-7*, *mut-14*, and found that levels of telomeric
292 siRNAs were sometimes depleted in these backgrounds, but not always (File S1).
293
294 Given that telomeric siRNAs are rare in small RNA sequencing data sets, we
295 hypothesized that loss of telomerase might elicit production of telomeric siRNAs in a
296 manner that might depend on Dicer. We therefore isolated RNA from wildtype control,
297 *trt-1* single mutant, and *trt-1; dcr-1* double mutant strains and prepared small RNA
298 libraries. We sequenced these libraries deeply in an effort to detect rare telomeric
299 siRNAs. We obtained ~20,000,000 reads each for 6 data sets and found that our *trt-1*
300 *dcr-1* data sets were strongly depleted of 22G RNAs that were previously reported to
301 depend on *dcr-1* (Figure S5A) (Gent et al., 2010). To assess TRT-1-dependent changes
302 in siRNAs throughout the genome, we counted the number of 22G reads mapping
303 uniquely antisense to protein-coding genes and found upregulation of siRNAs at 720
304 loci and downregulation at 456 loci in *trt-1* animals compared with wild-type (Figure
305 S5B). Of the upregulated loci, 465 were not upregulated in *trt-1; dcr-1* animals
306 compared with wild-type, indicating DCR-1 dependence. We did not find significant GO
307 terms in loci with either up or downregulated siRNA production. Given the importance of
308 both TRT-1 and siRNAs in germline function, we asked whether the loci with differential
309 siRNA production were enriched for germline-enriched genes. We used previously
310 published data on germline expression (Ortiz et al., 2014) and found significant
311 enrichment for germline-enriched genes in both upregulated and downregulated loci (p
312 $< 1e-19$ and $p < 1e-33$ respectively, Pearson's Chi Square test with Bonferroni
313 correction) (Figure S5C). This may reflect a form of epigenome dysregulation within
314 germ cells that occurs as a consequence of telomerase deficiency. siRNAs mapping to
315 transposons were unaffected by loss of TRT-1, with the exception of the CER-10 LTR
316 retrotransposon, for which siRNAs were three-fold downregulated (Figure S5D).
317

318 We detected no siRNAs composed of perfect telomere repeats in any genetic
319 background, but found some with up to 3 mismatches, whose levels did not change
320 substantially in siRNAs from *trt-1* single mutants or *trt-1; dcr-1* double mutants (Figure
321 4A). We next examined 22G RNAs at subtelomeric regions (defined as the 2kb of
322 sequence adjacent to the telomere) and found that these were present in wildtype
323 samples at the left end of chromosome III, and that their abundance was increased two-
324 fold in *trt-1* single mutants and their presence almost entirely eliminated in *trt-1; dcr-1*
325 double mutants (Figure 4C, E). Subtelomeric siRNAs were also observed within 1kb of
326 the telomere at the left ends of chromosomes *I* and *IV* in *trt-1* mutants and not in
327 wildtype or *trt-1; dcr-1* double mutants (Figure 4B, D). The right ends of Chromosomes *I*
328 and *III* and the left end of Chromosome *II* all showed at least a two-fold increase in
329 subtelomeric siRNAs in *trt-1* and/or *trt-1; dcr-1* double mutants (Figure 4E). We
330 observed a significant bias for subtelomeric siRNAs whose sequences correspond to
331 the C-rich telomere strand (antisense to TERRA) for the left arms of Chromosomes *I*
332 and *III* ($p < 1e-13$ and $p < 1e-43$ respectively, binomial test with Bonferroni correction)
333 and for the right arm of Chromosome *I* ($p < 1e-172$, binomial test with Bonferroni
334 correction) while the nucleotide sequences of subtelomeric siRNAs at the left arm of
335 Chromosome *IV* and the right arm of Chromosome *III* showed a bias for subtelomeric
336 TERRA, suggesting that they were created from ARRET ($p < 1e-11$, $p = 0.006$
337 respectively, binomial test with Bonferroni correction) (Figure 4F). These observations
338 suggest that telomere dysfunction triggers the upregulation of small RNA biogenesis at
339 multiple subtelomeres, through both DCR-1-dependent and -independent mechanisms.
340
341 We next studied data sets of small RNAs that immunoprecipitate with HRDE-1 and
342 WAGO-1, Argonaute proteins that promote silencing in the germline, as well as with the
343 germline anti-silencing Argonaute CSR-1 (Table S3). Enrichment of small RNAs for
344 each protein was calculated by dividing the number of reads in the immunoprecipitate
345 library by the number of reads in the corresponding input library. Telomeric siRNAs
346 were enriched in WAGO-1 immunoprecipates relative to input, but this was not the case
347 for HRDE-1 or CSR-1 (Figure 3G). Enrichment of subtelomeric small RNAs in WAGO-1
348 was detected at all chromosome ends tested apart from the right arm of Chromosome *I*

349 (some chromosome ends were not tested due to an absence of reads in the input
350 library). Enrichment was also detected for HRDE-1 at all chromosome ends excluding
351 the right arm of Chromosome *I* and the left arm of Chromosome *III* (Figure 3H).
352 Interestingly, CSR-1 showed the opposite pattern of enrichment to WAGO-1 and HRDE-
353 1, with enrichment at none of the chromosome ends apart from the right end of
354 Chromosome *I*. The ribosomal DNA, the most highly expressed locus in the *C. elegans*
355 genome, is immediately adjacent to this telomere (Wicky et al., 1996), and it is therefore
356 possible that siRNA activity takes a predominantly anti-silencing function at this
357 chromosome end. We asked if either Argonaute that associates with telomeric or sub-
358 telomeric siRNAs, WAGO-1 or to a lesser degree HRDE-1, promotes telomere
359 maintenance in the absence of telomerase and found that both *wago-1 trt-1* and *trt-1;*
360 *hrde-1* double mutants displayed rapid sterility phenotypes in comparison to *trt-1* single
361 mutants ($p < 1e-11$ and $p < 1e-12$, respectively, log rank test) (Figure 1E).
362
363 **Telomeric siRNAs and loss of EXO-1 repress sterility in the absence of**
364 **telomerase**
365 Although we failed to detect siRNAs with perfect telomere repeat sequence in our
366 siRNA data sets, these were present at very low levels in data sets generated by other
367 groups (Figure 3D-F) and could be difficult to detect for technical reasons. We
368 hypothesized that if loss of small RNAs directly targeting the telomere were responsible
369 for the rapid sterility in siRNA-deficient *trt-1*, then reintroduction of exogenous telomeric
370 siRNAs might rescue this phenotype. To address this experimentally, we used a viable
371 *dcr-1* allele, *mg375*, which is deficient for endogenous siRNA production but is
372 hypersensitive to exogenous RNAi when fed *E. coli* expressing dsRNA (Welker et al.,
373 2010). *trt-1; dcr-1(mg375)* double mutants that were passaged on bacteria expressing
374 telomeric dsRNA remained fertile significantly longer than those expressing dsRNA from
375 an empty vector control (Figure 4A). This delay of sterility did not occur for *trt-1* single
376 mutant controls. Moreover, *trt-1; dcr-1(mg375)* strains fed telomeric dsRNA had
377 markedly reduced levels of DNA damage at F6 in comparison to *trt-1; dcr-1(mg375)*
378 strains grown on control RNAi or on regular OP50 bacteria that do not express dsRNA
379 (Figure 1F, 5C).

380

381 In budding yeast, artificially-induced TERRA overexpression promotes telomere
382 shortening *in cis* by forming RNA:DNA hybrids that stall telomeric replication forks as
383 well as by stimulating telomeric resection by Exo1 (Maicher et al., 2012, Pfeiffer and
384 Lingner, 2012). We therefore hypothesized that loss of EXO-1 might rescue the
385 accelerated sterility phenotype in siRNA-deficient telomerase mutants. *trt-1; exo-1;*
386 *mut-14* triple mutant lines survived significantly longer than *trt-1; mut-14* double mutants
387 (Figure 5B) and showed reduced DNA damage and expression of moderate levels of
388 TERRA at F6 (Figures 5B, S5). Moreover, *trt-1; exo-1* double mutant controls remained
389 fertile even longer than *trt-1* single mutants (Figure 5B), indicating that EXO-1-mediated
390 resection promotes telomere-shortening-induced senescence in the absence of
391 telomerase, both at normal telomeres and at telomeres lacking siRNA-mediated
392 silencing. While *trt-1; exo-1* double mutant controls remained fertile longer than *trt-1*
393 single mutants, this was not true for *trt-1* single mutants grown on exogenous telomeric
394 dsRNA (Figure 5A, B). Thus, although loss of *exo-1* rescues the rapid sterility
395 phenotype in small RNA-deficient telomerase mutants, resection by EXO-1 also likely
396 promotes telomere shortening in *trt-1* single mutants independent of siRNA production
397 and telomeric heterochromatin structure.
398
399
400 **Discussion**
401
402 We propose the following model, based in part on our observations: upon telomere
403 shortening or damage, TERRA expression is transiently induced, which may recruit
404 telomerase (Moravec et al., 2016). If telomerase is present, shortened telomeres are
405 elongated. When telomerase is deficient, TERRA expression is suppressed via an
406 endogenous small RNA pathway that interacts with TERRA to facilitate telomeric
407 heterochromatin deposition. We observed upregulation of telomeric and subtelomeric
408 siRNAs in telomerase mutants, which may act as a negative feedback mechanism to
409 maintain appropriate levels of TERRA in the absence of telomerase. H3K9me2 but not
410 H3K9me3 is present at wildtype *C. elegans* telomeres, and we found that the *C.*

411 *elegans* HP1 homolog HPL-2 that binds to and specifically stabilizes H3K9me2
412 (McMurchy et al., 2017) represses telomere instability in the absence of telomerase. We
413 therefore propose that siRNAs function at naturally eroding telomeres to promote
414 heterochromatin formation in a manner that suppresses a form of replication-dependent
415 DNA damage that activates transcription of TERRA and associated small RNAs.
416 However, when small RNAs fail to promote heterochromatin formation at telomeres in
417 the absence of telomerase, our data suggest that EXO-1-mediated DNA damage then
418 leads to dysfunctional telomeres accompanied by high levels of TERRA that are
419 observed in early-generation *trt-1; dcr-1* double mutants (Figure 5). Importantly, loss of
420 EXO1 in telomerase-negative mice has been shown to extend lifespan and improve
421 organ maintenance by repressing ssDNA formation and the DNA damage response
422 (Schaetzlein et al., 2007), suggesting a conserved role for Exonuclease-1 in the
423 metazoan response to dysfunctional telomeres. It is possible that heterochromatin
424 creates a more compact telomere architecture that is resistant to nucleolytic attack by
425 EXO-1. Alternatively, damage signaling from eroding telomeres may recruit EXO-1 and
426 other DNA damage factors.
427
428 Our results demonstrating that high levels of TERRA are associated with telomere
429 instability might be consistent with a role for TERRA expression in the DNA damage
430 response as discussed by two recent studies. First, in mammals TERRA expression
431 occurs in response to a distinct form of telomeric damage - acutely deprotected, non-
432 replicating telomeres in the presence of telomerase – and is accompanied by production
433 of telomeric siRNAs that promote DNA damage response factor recruitment (Rossiello
434 et al., 2017). Second, a recent study in *S. cerevisiae* showed that increased TERRA
435 expression and persistent telomeric R-loops in telomerase mutants can repress
436 senescence by promoting recombination, indicating that increased levels of TERRA can
437 in some contexts be beneficial (Graf et al., 2017). Our observations that high levels of
438 TERRA are induced in telomerase negative small RNA mutants in response to EXO-1
439 (Figure 5), suggest that TERRA may be induced by or integral to a telomeric DNA
440 damage response.
441

442 We detected subtelomeric siRNAs that were dependent on Dicer and that interacted
443 with the Argonaute proteins WAGO-1 and HRDE-1 (Figure 3H), both of which promoted
444 telomere stability in the absence of telomerase. These Argonaute proteins are known to
445 be active in the germline and bind to RdRP-generated 22G RNAs that target
446 overlapping groups of transcripts, including genes, transposons and pseudogenes (Gu
447 et al., 2009). Moreover, WAGO-1 localizes to perinuclear P-granules (or germ
448 granules), where it could promote either transcriptional or post-transcriptional gene
449 silencing (Gu et al., 2009), whereas HRDE-1 is localized to the nucleus where it
450 promotes transcriptional gene silencing. The *C. elegans* Piwi homolog PRG-1 also
451 localizes to P granules, where it interacts with piRNAs to promote the biogenesis of
452 secondary 22G RNAs that may interact with HRDE-1 molecules that transiently enter P
453 granules before entering the nucleus to promote heterochromatin silencing. Moreover,
454 HRDE-1 and WAGO-1 have been shown to function redundantly to promote
455 transgenerational epigenomic silencing of transgenes, a form of permanent epigenomic
456 silencing that is initiated by PRG-1/Piwi and associated piRNAs (Ashe et al., 2012,
457 Buckley et al., 2012). Given that HRDE-1 and WAGO-1 interact with 22G siRNAs that
458 map to distinct and overlapping subtelomeres, we propose that these Argonaute
459 proteins collaborate to promote heterochromatin formation at subtelomeres, such that
460 both P-granule localized WAGO-1 and nuclear Argonaute HRDE-1 play important roles
461 in this silencing process. Although proteomics has been performed for both HRDE-1
462 and WAGO-1, these Argonaute proteins do not physically interact with one another or
463 possess common interacting proteins (Akay et al., 2017, Shirayama et al., 2014). We
464 propose that EXO-1-mediated telomere resection is accompanied by expression of
465 TERRA and ARRET, resulting in low levels of dsRNA that would elicit Dicer recruitment
466 via RDE-4 to create a primary siRNA population that would be amplified by RdRPs to
467 create 22G RNAs that associate with WAGO-1 and HRDE-1 to promote telomeric
468 silencing (Figure 6).
469
470 We did not detect any telomeric siRNAs lacking mismatches in our analysis of siRNAs
471 from telomerase mutants, nor could we identify Dicer-dependent telomeric siRNAs that
472 had mismatches. However, we did find that exogenous telomeric siRNAs were able to

473 complement the premature sterility of *trt-1 dcr-1* mutants (Figure 4A). Together, our
474 results suggest that while telomeric siRNAs can promote telomere stability in the
475 absence of telomerase, that subtelomeric transcripts are templates for *de novo*
476 synthesis of endogenous siRNAs that are relevant to telomere repeat stability.
477 Consistently, TERRA transcription in *S. pombe* initiates in the subtelomere but rarely
478 extends into the telomere (Moravec et al., 2016). We propose that TERRA is not
479 significantly expressed in RNAi deficient mutants that possess wildtype telomerase,
480 because telomerase is capable of healing telomeric damage that occurs in the absence
481 of small RNA-mediated heterochromatin formation.
482
483 Small RNAs promote genomic silencing of many types of transposons and are essential
484 for the stability of *Drosophila melanogaster* telomeres, which are composed of non-LTR
485 retrotransposons that are distinct from the simple repetitive sequences that are
486 maintained by telomerase and cap chromosome ends in most organisms (Pardue and
487 DeBaryshe, 2003). siRNAs function at *Drosophila* telomeres to promote
488 heterochromatin-mediated genome silencing via the *Drosophila* homologs of HP1 and
489 ATRX, thereby preventing telomere instability (Chavez et al., 2017, Fulcher et al.,
490 2014). Small RNA-mediated control of telomere stability through regulation of
491 heterochromatin is therefore a conserved feature of both non-canonical and canonical
492 telomeres. siRNA dysfunction at *Drosophila* telomeres leads to immediate telomere
493 deprotection and fusion in embryos, whereas *C. elegans* siRNA mutants telomeres
494 have normal lengths (Figure S1). When both telomerase and *C. elegans* siRNA factors
495 are removed, telomeres trigger a DNA damage response in many germ cells but this
496 does not result in telomere fusions for several generations, each generation
497 representing 8-10 cell divisions. This indicates that the accelerated sterility phenotype of
498 siRNA-deficient *trt-1* mutants is not a consequence of a defect in acute telomere
499 uncapping, but rather an acceleration of the onset of crisis. We speculate siRNA-
500 mediated heterochromatin formation at telomeres modulates the stability of telomeres in
501 diverse organisms that maintain their telomeres via telomerase-mediated telomere
502 repeat addition.
503

504 Since most human somatic cells do not express telomerase, our findings may be
505 generally relevant to understanding how cells control the rate of telomere shortening in
506 the absence of telomerase through modulation of telomeric transcription and chromatin
507 either in the germ cells, in the early embryo or in adult somatic cells. Increased TERRA
508 expression and telomeric R-loops have been reported to associate with high levels of
509 DNA damage in ICF syndrome cells, which are deficient for DNA methylation at
510 repetitive segments of the genome, including telomeres, and undergo rapid telomere
511 shortening and senescence (Sagie et al., 2017). As telomeric damage associated with
512 senescence can induce broad changes to chromatin and histone biosynthesis
513 (O'Sullivan et al., 2010), and our data suggest that the reverse may also be true; global
514 dysfunction of the epigenome, which may be a hallmark of human aging (Zhang et al.,
515 2015), could elicit rapid telomere instability and irreversible damage in cells that are
516 deficient for telomerase. We propose that small RNAs could be generally relevant to
517 lncRNA-mediated heterochromatin formation at telomeres and possibly elsewhere in the
518 genome, such as loci that are subjected to parent-of-origin genomic imprinting (Holoch
519 and Moazed, 2015, Taylor et al., 2015).
520
521 Finally, we note that the *C. elegans* secondary siRNA biogenesis factor MUT-7 (Figure
522 1A, B) is homologous to the exonuclease domain of human WRN1, which is commonly
523 mutated in Werner's syndrome and results in early-onset aging of multiple tissues.
524 WRN1 deficiency is accompanied by accelerated telomere erosion and senescence
525 phenotypes that can be rescued by telomerase expression (Shimamoto et al., 2015).
526 While WRN1 and its homologs have been intensively studied for their roles in DNA
527 recombination, WRN1 was recently shown to safeguard the epigenomic stability of
528 heterochromatin (Zhang et al., 2015). Our study suggests that Werner syndrome may
529 be explained, in part, by defects in siRNA-mediated heterochromatin silencing at
530 telomeres and elsewhere in the genome.
531
532
533
534

535 **Materials and Methods**
536

537 Strains: Unless otherwise noted, all strains were maintained at 20°C on nematode
538 growth medium plates seeded with *Escherichia coli* OP50. Strains used include Bristol
539 N2 ancestral, *wago-1(tm1414)*, *trt-1(ok410), unc-29(e193), dpy-5(e61), dcr-1(mg375),*
540 *hrde-1(tm1200), rde-1(ne219), rde-4(ne299), rrf-3(mg373), rrf-2(ok210), eri-1(mg366),*
541 *mut-7(pk204), mut-7(pk720), mut-14(pk738), rbr-2(tm1231), spr-5(by101), xnp-*
542 *1(ok1823), xnp-1(tm678), hpl-1(tm1624), hpl-2(ok916), hpl-2(tm1479), exo-1(tm1842)*.
543 A *trt-1 unc-29* double mutant, where *unc-29* is tightly linked to *trt-1*, was used to create
544 strains used in this study. Double, triple and quadruple mutants were created using
545 standard marker mutations and verified based on phenotype or genotype.

546 DAPI staining: One-day-old adults were washed twice in M9, soaked in 150 µL of
547 400ng/mL DAPI in ethanol solution for 30 min or until evaporated, rehydrated in 2 mL of
548 M9 solution overnight at 4°C, and mounted in 8 µL VECTASHIELD mounting medium
549 (Vector Laboratories). Chromosome counts were performed under 60x magnification
550 and a 359nm excitation wavelength using a Nikon Eclipse E800 microscope.

551 qPCR: Non-starved mixed-stage worms were washed with M9 and RNA was extracted
552 using 1 mL TRIZOL according to the manufacturer's instructions. For RT-PCR analysis,
553 total RNA was treated twice with DNase I and was reverse transcribed with act-1 and a
554 telomere-specific primer ($(GCCTAA)_3$) using SuperScript II reverse transcriptase
555 (Invitrogen). For SYBR green reactions, subtelomere specific primers were designed
556 within 200bp of the telomere-subtelomere junction.
557

558 RNA FISH: RNA FISH was performed as previously described (Sakaguchi et al., 2014)
559 with several modifications. In brief, non-starved, mixed-stage animals were washed
560 twice in M9 and three times in 1x DEPC-treated PBS. Worms were fixed in 1mL
561 fixation buffer (1x DEPC-treated PBS with 3.7% formaldehyde) for 45 min rotating at
562 room temperature then washed twice in 1mL 1x DEPC-treated PBS. Fixed animals
563 were permeabilized overnight at 4°C in 70% ethanol in DEPC-treated H_2O, then washed
564 in 1 mL wash buffer [10% (vol/vol) formamide in 2x RNases-free SSC]. Aliquots of each

565 sample were removed prior to hybridization and treated with RNaseA for 1h at 37°C to
566 ensure probe specificity to RNA. Hybridization was performed at 30°C overnight in 100
567 µL hybridization buffer (10% dextran sulfate, 2x RNase-free SSC, 10% deionized
568 formamide, 50, 0.02% RNase-free BSA, 50 µg *E. coli* tRNA) with 1.25 µM probe. Cy5-
569 labelled $(GCCTAA)_3$ probe was used to detect TERRA transcripts. Animals were
570 washed twice with wash buffer, counterstained with 25 ng/mL DAPI for 30 min at room
571 temperature, and mounted on glass slides in VECTASHIELD mounting medium (Vector
572 Laboratories) before epifluorescence microscopy.
573
574 IF: IF was carried out as previously described (Phillips et al., 2009) by fixing dissected
575 gonads of 1 day old adults in 2% PFA for 10 minutes followed by a 1 minute postfixation
576 in methanol. Rabbit anti-pS/TQ (Cell Signaling Technology) was used at a 1:500 dilution
577 and mouse anti-RNA:DNA hybrid S9.6 at 1:500 dilution. Stained gonads were
578 counterstained with DAPI and mounted with VECTASHIELD (Vector laboratories)
579 before epifluorescence microscopy.
580
581 RNAi: RNAi clone expressing dsRNA targeting *C. elegans* telomeres was constructed
582 using NEB HiFi DNA assembly mix according to the manufacturer's instructions. 200
583 bp of telomeric repeats were amplified from cTel55x by PCR with 20 bp overlap to SpeI
584 digested L4440. Correct constructs were transformed into HT115 and RNAi was
585 performed as previously described (McMurchy et al., 2017).
586
587 Southern Blot: *C. elegans* genomic DNA was digested overnight with Hinf1 (New
588 England Biolabs), separated on a 0.8% agarose gel at 1.5 V/cm, and transferred to a
589 neutral nylon membrane (Hybond-N, GE Healthcare Life Sciences). A digoxigenin-
590 labelled telomere probe was hybridized and detected as described (Ahmed and
591 Hodgkin, 2000).
592
593 Mrt and ALT assays: When telomerase-deficient *trt-1(ok410) C. elegans* mutants are
594 passaged by using the standard Mortal Germline (Mrt) assay developed in our
595 laboratory, which involves passaging six L1 larval animals to fresh plates weekly, 100%

596 become sterile within 20–30 generations. When *trt-1(ok410)* strains are passaged
597 weekly by transferring a 1cm^2 chunk of agar populated with ≈200–400 animals, 10-20%
598 of the strains survive for hundreds of generations. Mantel-Cox Log Rank Analysis was
599 used to determine differences of transgenerational lifespan between strains. A z-test
600 was performed to compare proportion of ALT survivors in chunked strains.
601
602 RNA-seq: Animals were grown at 20°C on 100 mm NGM plates seeded with OP50
603 bacteria. Two biological replicates were prepared for each genotype. RNA was
604 extracted using Trizol (Ambion) followed by isopropanol precipitation. RNA samples
605 were treated with 20U RNA 5' polyphosphatase (Lucigen, RP8092H) for 30 minutes at
606 37°C to remove 5' triphosphate groups. Library preparation and sequencing was
607 performed at the UNC School of Medicine High-Throughput Sequencing Facility
608 (HTSF). RNA-seq libraries were prepared using the NEXTflex Small RNA Library Prep
609 Kit for Illumina (Bio Scientific). Libraries were sequenced on an Illumina HiSeq 2500 to
610 produce approximately twenty million 50 bp single-end reads per library.
611
612 Analysis of high throughput sequencing data: Publicly available RNA-seq datasets were
613 download from the Gene Expression Omnibus (https://www.ncbi.nlm.nih.gov/geo/) (see
614 table X for library information). Adapter trimming was performed as required using the
615 bbduk.sh script from the bbmap suite3 and custom scripts (Bushnell, 2016). Reads were
616 then filtered for 22G species or all species between 18 and 30 nucleotides in length
617 using a custom python script. Reads were then converted to fasta format and mapped
618 to the *C. elegans* genome (WS251) using bowtie (Langmead et al., 2009) with the
619 following options: -M 1 -v 0 -best -strata. Uniquely mapping siRNAs were detected by
620 replacing the -M 1 parameter with -m 1. To detect telomere-mapping sRNAs, reads
621 were mapped to seven repeats of perfect telomere sequence (TTAGGC), allowing for
622 zero mismatches. Unmapped reads were re-mapped to the telomere sequence, this
623 time allowing for one mismatch. This step was repeated to detect reads that map to
624 telomeres with two or three mismatches. Genes with differential siRNA abundance in *trt-*
625 *1* were identified using DESeq2 (Love et al., 2014). To detect changes in the
626 abundance of subtelomeric siRNAs in *trt-1* and *trt-1; dcr-1*, 22G reads mapping to the

627 2kb of sequence adjacent to the telomere were counted for each chromosome arm.
628 Counts were normalized by dividing by the total number of mapped reads for each
629 library. A pseudocount of 1 was added to each normalized value to avoid division by
630 zero errors. Replicates were averaged and the log2-fold change between mutant and
631 wild-type was calculated for each subtelomere. Analysis of sequencing data was
632 performed using the R statistical computing environment (Team, 2017). Genome
633 regions were visualized using the Gviz R package (Hahne and Ivanek, 2016).
634 Immunoprecipitation datasets were used in Figure 3G, H but were excluded from the
635 analysis shown in Figure 3D-F. To detected siRNAs targeting transposons, 22G reads
636 were mapped to the *C. elegans* transposon consensus sequences downloaded from
637 Repbase with bowtie, allowing for up to two mismatches.
638 ChIP-seq reads were mapped to the genome as fastq files as described above without
639 the size filtering step. Read coverage was calculated at each base using bedtools
640 (Quinlan and Hall, 2010). Coverage values were normalized by dividing by the number
641 of total mapped reads for each library and enrichment was calculated by dividing the
642 normalized coverage for I.P. libraries by the normalized coverage of their respective
643 input libraries.
644
645 Accession numbers: RNA-seq data reported in this study are available under the
646 accession number GEO: GSE111800.
647
648 **Acknowledgements**
649 We thank R. Dowen for technical advice with qRT-PCR, K. Billmyre for advice on
650 immunofluorescence, and members of the S.A. laboratory for critical review of the
651 manuscript. Some strains were provided by the Caenorhabditis Genetics Center, which
652 is funded by National Institutes of Health Office of Research Infrastructure Programs
653 (P40 OD010440). S.F., C.L. and S.A. were supported by National Institute of Health
654 grant R01 GM066228.
655
656 **Competing Interests**
657 The authors declare no competing interests.

658 **References**
659

660 AHMED, S. & HODGKIN, J. 2000. MRT-2 checkpoint protein is required for germline
661 immortality and telomere replication in *C. elegans*. *Nature,* 403**,** 159-64.
662 AKAY, A., DI DOMENICO, T., SUEN, K. M., NABIH, A., PARADA, G. E., LARANCE,
663 M., MEDHI, R., BERKYUREK, A. C., ZHANG, X., WEDELES, C. J., RUDOLPH,
664 K. L. M., ENGELHARDT, J., HEMBERG, M., MA, P., LAMOND, A. I.,
665 CLAYCOMB, J. M. & MISKA, E. A. 2017. The Helicase Aquarius/EMB-4 Is
666 Required to Overcome Intronic Barriers to Allow Nuclear RNAi Pathways to
667 Heritably Silence Transcription. *Dev Cell,* 42**,** 241-255 e6.
668 ARNOULT, N., VAN BENEDEN, A. & DECOTTIGNIES, A. 2012. Telomere length
669 regulates TERRA levels through increased trimethylation of telomeric H3K9 and
670 HP1alpha. *Nat Struct Mol Biol,* 19**,** 948-56.
671 ASHE, A., SAPETSCHNIG, A., WEICK, E. M., MITCHELL, J., BAGIJN, M. P.,
672 CORDING, A. C., DOEBLEY, A. L., GOLDSTEIN, L. D., LEHRBACH, N. J., LE
673 PEN, J., PINTACUDA, G., SAKAGUCHI, A., SARKIES, P., AHMED, S. & MISKA,
674 E. A. 2012. piRNAs Can Trigger a Multigenerational Epigenetic Memory in the
675 Germline of C. elegans. *Cell,* 150**,** 88-99.
676 AVGOUSTI, D. C., PALANI, S., SHERMAN, Y. & GRISHOK, A. 2012. CSR-1 RNAi
677 pathway positively regulates histone expression in C. elegans. *EMBO J,* 31**,**
678 3821-32.
679 AZZALIN, C. M. & LINGNER, J. 2015. Telomere functions grounding on TERRA firma.
680 *Trends Cell Biol,* 25**,** 29-36.
681 AZZALIN, C. M., REICHENBACH, P., KHORIAULI, L., GIULOTTO, E. & LINGNER, J.
682 2007. Telomeric repeat containing RNA and RNA surveillance factors at
683 mammalian chromosome ends. *Science,* 318**,** 798-801.
684 BAGIJN, M. P., GOLDSTEIN, L. D., SAPETSCHNIG, A., WEICK, E. M., BOUASKER,
685 S., LEHRBACH, N. J., SIMARD, M. J. & MISKA, E. A. 2012. Function, targets,
686 and evolution of Caenorhabditis elegans piRNAs. *Science,* 337**,** 574-8.
687 BATISTA, P. J., RUBY, J. G., CLAYCOMB, J. M., CHIANG, R., FAHLGREN, N.,
688 KASSCHAU, K. D., CHAVES, D. A., GU, W., VASALE, J. J., DUAN, S., CONTE,
689 D., JR., LUO, S., SCHROTH, G. P., CARRINGTON, J. C., BARTEL, D. P. &
690 MELLO, C. C. 2008. PRG-1 and 21U-RNAs interact to form the piRNA complex
691 required for fertility in C. elegans. *Mol Cell,* 31**,** 67-78.
692 BENETTI, R., GARCIA-CAO, M. & BLASCO, M. A. 2007. Telomere length regulates the
693 epigenetic status of mammalian telomeres and subtelomeres. *Nat Genet,* 39**,**
694 243-50.
695 BENETTI, R., SCHOEFTNER, S., MUNOZ, P. & BLASCO, M. A. 2008. Role of TRF2 in
696 the assembly of telomeric chromatin. *Cell Cycle,* 7**,** 3461-8.
697 BERNSTEIN, E., CAUDY, A. A., HAMMOND, S. M. & HANNON, G. J. 2001. Role for a
698 bidentate ribonuclease in the initiation step of RNA interference. *Nature,* 409**,**
699 363-6.
700 BILLI, A. C., FISCHER, S. E. & KIM, J. K. 2014. Endogenous RNAi pathways in C.
701 elegans. *WormBook***,** 1-49.
702 BUCKLEY, B. A., BURKHART, K. B., GU, S. G., SPRACKLIN, G., KERSHNER, A.,
703 FRITZ, H., KIMBLE, J., FIRE, A. & KENNEDY, S. 2012. A nuclear Argonaute

704 promotes multigenerational epigenetic inheritance and germline immortality.
705 *Nature,* 489**,** 447-51.
706 BUSHNELL, B. 2016. BBMap short-read aligner, and other bioinformatics tools.
707 http://sourceforge.net/projects/bbmap/.
708 CANZIO, D., LARSON, A. & NARLIKAR, G. J. 2014. Mechanisms of functional
709 promiscuity by HP1 proteins. *Trends Cell Biol,* 24**,** 377-86.
710 CAO, F., LI, X., HIEW, S., BRADY, H., LIU, Y. & DOU, Y. 2009. Dicer independent
711 small RNAs associate with telomeric heterochromatin. *RNA,* 15**,** 1274-81.
712 CHAVEZ, J., MURILLO-MALDONADO, J. M., BAHENA, V., CRUZ, A. K.,
713 CASTANEDA-SORTIBRAN, A., RODRIGUEZ-ARNAIZ, R., ZURITA, M. &
714 VALADEZ-GRAHAM, V. 2017. dAdd1 and dXNP prevent genome instability by
715 maintaining HP1a localization at Drosophila telomeres. *Chromosoma,* 126**,** 697-
716 712.
717 CHENG, C., SHTESSEL, L., BRADY, M. M. & AHMED, S. 2012. Caenorhabditis
718 elegans POT-2 telomere protein represses a mode of alternative lengthening of
719 telomeres with normal telomere lengths. *Proc Natl Acad Sci U S A,* 109**,** 7805-10.
720 CUSANELLI, E., ROMERO, C. A. & CHARTRAND, P. 2013. Telomeric noncoding RNA
721 TERRA is induced by telomere shortening to nucleate telomerase molecules at
722 short telomeres. *Mol Cell,* 51**,** 780-91.
723 DAS, P. P., BAGIJN, M. P., GOLDSTEIN, L. D., WOOLFORD, J. R., LEHRBACH, N. J.,
724 SAPETSCHNIG, A., BUHECHA, H. R., GILCHRIST, M. J., HOWE, K. L.,
725 STARK, R., MATTHEWS, N., BEREZIKOV, E., KETTING, R. F., TAVARE, S. &
726 MISKA, E. A. 2008. Piwi and piRNAs act upstream of an endogenous siRNA
727 pathway to suppress Tc3 transposon mobility in the Caenorhabditis elegans
728 germline. *Mol Cell,* 31**,** 79-90.
729 DONATE, L. E. & BLASCO, M. A. 2011. Telomeres in cancer and ageing. *Philos Trans*
730 *R Soc Lond B Biol Sci,* 366**,** 76-84.
731 FLYNN, R. L., COX, K. E., JEITANY, M., WAKIMOTO, H., BRYLL, A. R., GANEM, N.
732 J., BERSANI, F., PINEDA, J. R., SUVA, M. L., BENES, C. H., HABER, D. A.,
733 BOUSSIN, F. D. & ZOU, L. 2015. Alternative lengthening of telomeres renders
734 cancer cells hypersensitive to ATR inhibitors. *Science,* 347**,** 273-7.
735 FULCHER, N., DERBOVEN, E., VALUCHOVA, S. & RIHA, K. 2014. If the cap fits, wear
736 it: an overview of telomeric structures over evolution. *Cell Mol Life Sci,* 71**,** 847-
737 65.
738 GENT, J. I., LAMM, A. T., PAVELEC, D. M., MANIAR, J. M., PARAMESWARAN, P.,
739 TAO, L., KENNEDY, S. & FIRE, A. Z. 2010. Distinct phases of siRNA synthesis
740 in an endogenous RNAi pathway in C. elegans soma. *Mol Cell,* 37**,** 679-89.
741 GOU, L. T., DAI, P., YANG, J. H., XUE, Y., HU, Y. P., ZHOU, Y., KANG, J. Y., WANG,
742 X., LI, H., HUA, M. M., ZHAO, S., HU, S. D., WU, L. G., SHI, H. J., LI, Y., FU, X.
743 D., QU, L. H., WANG, E. D. & LIU, M. F. 2014. Pachytene piRNAs instruct
744 massive mRNA elimination during late spermiogenesis. *Cell Res,* 24**,** 680-700.
745 GRAF, M., BONETTI, D., LOCKHART, A., SERHAL, K., KELLNER, V., MAICHER, A.,
746 JOLIVET, P., TEIXEIRA, M. T. & LUKE, B. 2017. Telomere Length Determines
747 TERRA and R-Loop Regulation through the Cell Cycle. *Cell,* 170**,** 72-85 e14.
748 GREER, E. L., MAURES, T. J., HAUSWIRTH, A. G., GREEN, E. M., LEEMAN, D. S.,
749 MARO, G. S., HAN, S., BANKO, M. R., GOZANI, O. & BRUNET, A. 2010.

750 Members of the H3K4 trimethylation complex regulate lifespan in a germline-
751 dependent manner in C. elegans. *Nature,* 466**,** 383-7.
752 GU, W., SHIRAYAMA, M., CONTE, D., JR., VASALE, J., BATISTA, P. J., CLAYCOMB,
753 J. M., MORESCO, J. J., YOUNGMAN, E. M., KEYS, J., STOLTZ, M. J., CHEN,
754 C. C., CHAVES, D. A., DUAN, S., KASSCHAU, K. D., FAHLGREN, N., YATES,
755 J. R., 3RD, MITANI, S., CARRINGTON, J. C. & MELLO, C. C. 2009. Distinct
756 argonaute-mediated 22G-RNA pathways direct genome surveillance in the C.
757 elegans germline. *Mol Cell,* 36**,** 231-44.
758 HAHNE, F. & IVANEK, R. 2016. Visualizing Genomic Data Using Gviz and
759 Bioconductor. *Methods Mol Biol,* 1418**,** 335-51.
760 HAN, T., MANOHARAN, A. P., HARKINS, T. T., BOUFFARD, P., FITZPATRICK, C.,
761 CHU, D. S., THIERRY-MIEG, D., THIERRY-MIEG, J. & KIM, J. K. 2009. 26G
762 endo-siRNAs regulate spermatogenic and zygotic gene expression in
763 Caenorhabditis elegans. *Proc Natl Acad Sci U S A,* 106**,** 18674-9.
764 HEARD, E. & TURNER, J. 2011. Function of the sex chromosomes in mammalian
765 fertility. *Cold Spring Harb Perspect Biol,* 3**,** a002675.
766 HOLOCH, D. & MOAZED, D. 2015. RNA-mediated epigenetic regulation of gene
767 expression. *Nat Rev Genet,* 16**,** 71-84.
768 HOLOHAN, B., WRIGHT, W. E. & SHAY, J. W. 2014. Cell biology of disease:
769 Telomeropathies: an emerging spectrum disorder. *J Cell Biol,* 205**,** 289-99.
770 KETTING, R. F., FISCHER, S. E., BERNSTEIN, E., SIJEN, T., HANNON, G. J. &
771 PLASTERK, R. H. 2001. Dicer functions in RNA interference and in synthesis of
772 small RNA involved in developmental timing in C. elegans. *Genes Dev,* 15**,** 2654-
773 9.
774 KETTING, R. F., HAVERKAMP, T. H., VAN LUENEN, H. G. & PLASTERK, R. H. 1999.
775 Mut-7 of C. elegans, required for transposon silencing and RNA interference, is a
776 homolog of Werner syndrome helicase and RNaseD. *Cell,* 99**,** 133-41.
777 KNIGHT, S. W. & BASS, B. L. 2001. A role for the RNase III enzyme DCR-1 in RNA
778 interference and germ line development in Caenorhabditis elegans. *Science,*
779 293**,** 2269-71.
780 LANGMEAD, B., TRAPNELL, C., POP, M. & SALZBERG, S. L. 2009. Ultrafast and
781 memory-efficient alignment of short DNA sequences to the human genome.
782 *Genome Biol,* 10**,** R25.
783 LI, F., HUARTE, M., ZARATIEGUI, M., VAUGHN, M. W., SHI, Y., MARTIENSSEN, R. &
784 CANDE, W. Z. 2008. Lid2 is required for coordinating H3K4 and H3K9
785 methylation of heterochromatin and euchromatin. *Cell,* 135**,** 272-83.
786 LI, J. S., MIRALLES FUSTE, J., SIMAVORIAN, T., BARTOCCI, C., TSAI, J.,
787 KARLSEDER, J. & LAZZERINI DENCHI, E. 2017. TZAP: A telomere-associated
788 protein involved in telomere length control. *Science,* 355**,** 638-641.
789 LOVE, M. I., HUBER, W. & ANDERS, S. 2014. Moderated estimation of fold change
790 and dispersion for RNA-seq data with DESeq2. *Genome Biol,* 15**,** 550.
791 LOVEJOY, C. A., LI, W., REISENWEBER, S., THONGTHIP, S., BRUNO, J., DE
792 LANGE, T., DE, S., PETRINI, J. H., SUNG, P. A., JASIN, M., ROSENBLUH, J.,
793 ZWANG, Y., WEIR, B. A., HATTON, C., IVANOVA, E., MACCONAILL, L.,
794 HANNA, M., HAHN, W. C., LUE, N. F., REDDEL, R. R., JIAO, Y., KINZLER, K.,
795 VOGELSTEIN, B., PAPADOPOULOS, N., MEEKER, A. K. & CONSORTIUM, A.

L. T. S. C. 2012. Loss of ATRX, genome instability, and an altered DNA damage response are hallmarks of the alternative lengthening of telomeres pathway. *PLoS Genet,* 8**,** e1002772.

MACIEJOWSKI, J. & DE LANGE, T. 2017. Telomeres in cancer: tumour suppression and genome instability. *Nat Rev Mol Cell Biol,* 18**,** 175-186.

MAICHER, A., KASTNER, L., DEES, M. & LUKE, B. 2012. Deregulated telomere transcription causes replication-dependent telomere shortening and promotes cellular senescence. *Nucleic Acids Res,* 40**,** 6649-59.

MCMURCHY, A. N., STEMPOR, P., GAARENSTROOM, T., WYSOLMERSKI, B., DONG, Y., AUSSIANIKAVA, D., APPERT, A., HUANG, N., KOLASINSKA-ZWIERZ, P., SAPETSCHNIG, A., MISKA, E. A. & AHRINGER, J. 2017. A team of heterochromatin factors collaborates with small RNA pathways to combat repetitive elements and germline stress. *Elife,* 6.

MORAVEC, M., WISCHNEWSKI, H., BAH, A., HU, Y., LIU, N., LAFRANCHI, L., KING, M. C. & AZZALIN, C. M. 2016. TERRA promotes telomerase-mediated telomere elongation in Schizosaccharomyces pombe. *EMBO Rep,* 17**,** 999-1012.

O'SULLIVAN, R. J., KUBICEK, S., SCHREIBER, S. L. & KARLSEDER, J. 2010. Reduced histone biosynthesis and chromatin changes arising from a damage signal at telomeres. *Nat Struct Mol Biol,* 17**,** 1218-25.

ORTIZ, M. A., NOBLE, D., SOROKIN, E. P. & KIMBLE, J. 2014. A new dataset of spermatogenic vs. oogenic transcriptomes in the nematode Caenorhabditis elegans. *G3 (Bethesda),* 4**,** 1765-72.

PAK, J. & FIRE, A. 2007. Distinct populations of primary and secondary effectors during RNAi in C. elegans. *Science,* 315**,** 241-4.

PARDUE, M. L. & DEBARYSHE, P. G. 2003. Retrotransposons provide an evolutionarily robust non-telomerase mechanism to maintain telomeres. *Annu Rev Genet,* 37**,** 485-511.

PFEIFFER, V. & LINGNER, J. 2012. TERRA promotes telomere shortening through exonuclease 1-mediated resection of chromosome ends. *PLoS Genet,* 8**,** e1002747.

PHILLIPS, C. M., MCDONALD, K. L. & DERNBURG, A. F. 2009. Cytological analysis of meiosis in Caenorhabditis elegans. *Methods Mol Biol,* 558**,** 171-95.

PICKETT, H. A. & REDDEL, R. R. 2015. Molecular mechanisms of activity and derepression of alternative lengthening of telomeres. *Nat Struct Mol Biol,* 22**,** 875-80.

PORRO, A., FEUERHAHN, S., DELAFONTAINE, J., RIETHMAN, H., ROUGEMONT, J. & LINGNER, J. 2014. Functional characterization of the TERRA transcriptome at damaged telomeres. *Nat Commun,* 5**,** 5379.

QUINLAN, A. R. & HALL, I. M. 2010. BEDTools: a flexible suite of utilities for comparing genomic features. *Bioinformatics,* 26**,** 841-2.

REINHART, B. J. & BARTEL, D. P. 2002. Small RNAs correspond to centromere heterochromatic repeats. *Science,* 297**,** 1831.

ROSSIELLO, F., AGUADO, J., SEPE, S., IANNELLI, F., NGUYEN, Q., PITCHIAYA, S., CARNINCI, P. & D'ADDA DI FAGAGNA, F. 2017. DNA damage response inhibition at dysfunctional telomeres by modulation of telomeric DNA damage response RNAs. *Nat Commun,* 8**,** 13980.

842 SAGIE, S., TOUBIANA, S., HARTONO, S. R., KATZIR, H., TZUR-GILAT, A.,
843 HAVAZELET, S., FRANCASTEL, C., VELASCO, G., CHEDIN, F. & SELIG, S.
844 2017. Telomeres in ICF syndrome cells are vulnerable to DNA damage due to
845 elevated DNA:RNA hybrids. *Nat Commun,* 8**,** 14015.
846 SAKAGUCHI, A., SARKIES, P., SIMON, M., DOEBLEY, A. L., GOLDSTEIN, L. D.,
847 HEDGES, A., IKEGAMI, K., ALVARES, S. M., YANG, L., LAROCQUE, J. R.,
848 HALL, J., MISKA, E. A. & AHMED, S. 2014. Caenorhabditis elegans RSD-2 and
849 RSD-6 promote germ cell immortality by maintaining small interfering RNA
850 populations. *Proc Natl Acad Sci U S A,* 111**,** E4323-31.
851 SCHAETZLEIN, S., KODANDARAMIREDDY, N. R., JU, Z., LECHEL, A.,
852 STEPCZYNSKA, A., LILLI, D. R., CLARK, A. B., RUDOLPH, C., KUHNEL, F.,
853 WEI, K., SCHLEGELBERGER, B., SCHIRMACHER, P., KUNKEL, T. A.,
854 GREENBERG, R. A., EDELMANN, W. & RUDOLPH, K. L. 2007. Exonuclease-1
855 deletion impairs DNA damage signaling and prolongs lifespan of telomere-
856 dysfunctional mice. *Cell,* 130**,** 863-77.
857 SHAY, J. W. 2016. Role of Telomeres and Telomerase in Aging and Cancer. *Cancer*
858 *Discov,* 6**,** 584-93.
859 SHIMAMOTO, A., YOKOTE, K. & TAHARA, H. 2015. Werner Syndrome-specific
860 induced pluripotent stem cells: recovery of telomere function by reprogramming.
861 *Front Genet,* 6**,** 10.
862 SHIRAYAMA, M., STANNEY, W., 3RD, GU, W., SETH, M. & MELLO, C. C. 2014. The
863 Vasa Homolog RDE-12 engages target mRNA and multiple argonaute proteins to
864 promote RNAi in C. elegans. *Curr Biol,* 24**,** 845-51.
865 STEINER, F. A., OKIHARA, K. L., HOOGSTRATE, S. W., SIJEN, T. & KETTING, R. F.
866 2009. RDE-1 slicer activity is required only for passenger-strand cleavage during
867 RNAi in Caenorhabditis elegans. *Nat Struct Mol Biol,* 16**,** 207-11.
868 TABARA, H., YIGIT, E., SIOMI, H. & MELLO, C. C. 2002. The dsRNA binding protein
869 RDE-4 interacts with RDE-1, DCR-1, and a DExH-box helicase to direct RNAi in
870 C. elegans. *Cell,* 109**,** 861-71.
871 TAYLOR, D. H., CHU, E. T., SPEKTOR, R. & SOLOWAY, P. D. 2015. Long non-coding
872 RNA regulation of reproduction and development. *Mol Reprod Dev,* 82**,** 932-56.
873 TEAM, R. C. 2017. R: A language and environment for statistical computing. R
874 Foundation for Statistical Computing, Vienna, Austria. https://www.R-project.org/.
875 TIJSTERMAN, M., KETTING, R. F., OKIHARA, K. L., SIJEN, T. & PLASTERK, R. H.
876 2002. RNA helicase MUT-14-dependent gene silencing triggered in C. elegans
877 by short antisense RNAs. *Science,* 295**,** 694-7.
878 UDUGAMA, M., FT, M. C., CHAN, F. L., TANG, M. C., PICKETT, H. A., JD, R. M.,
879 MAYNE, L., COLLAS, P., MANN, J. R. & WONG, L. H. 2015. Histone variant
880 H3.3 provides the heterochromatic H3 lysine 9 tri-methylation mark at telomeres.
881 *Nucleic Acids Res,* 43**,** 10227-37.
882 VRBSKY, J., AKIMCHEVA, S., WATSON, J. M., TURNER, T. L., DAXINGER, L.,
883 VYSKOT, B., AUFSATZ, W. & RIHA, K. 2010. siRNA-mediated methylation of
884 Arabidopsis telomeres. *PLoS Genet,* 6**,** e1000986.
885 WEDELES, C. J., WU, M. Z. & CLAYCOMB, J. M. 2013. Protection of germline gene
886 expression by the C. elegans Argonaute CSR-1. *Dev Cell,* 27**,** 664-71.

887 WELKER, N. C., PAVELEC, D. M., NIX, D. A., DUCHAINE, T. F., KENNEDY, S. &
888 BASS, B. L. 2010. Dicer's helicase domain is required for accumulation of some,
889 but not all, C. elegans endogenous siRNAs. *RNA,* 16**,** 893-903.
890 WICKY, C., VILLENEUVE, A. M., LAUPER, N., CODOUREY, L., TOBLER, H. &
891 MULLER, F. 1996. Telomeric repeats (TTAGGC)n are sufficient for chromosome
892 capping function in Caenorhabditis elegans. *Proc Natl Acad Sci U S A,* 93**,** 8983-
893 8.
894 WONG, L. H., MCGHIE, J. D., SIM, M., ANDERSON, M. A., AHN, S., HANNAN, R. D.,
895 GEORGE, A. J., MORGAN, K. A., MANN, J. R. & CHOO, K. H. 2010. ATRX
896 interacts with H3.3 in maintaining telomere structural integrity in pluripotent
897 embryonic stem cells. *Genome Res,* 20**,** 351-60.
898 ZELLER, P., PADEKEN, J., VAN SCHENDEL, R., KALCK, V., TIJSTERMAN, M. &
899 GASSER, S. M. 2016. Histone H3K9 methylation is dispensable for
900 Caenorhabditis elegans development but suppresses RNA:DNA hybrid-
901 associated repeat instability. *Nat Genet,* 48**,** 1385-1395.
902 ZHANG, W., LI, J., SUZUKI, K., QU, J., WANG, P., ZHOU, J., LIU, X., REN, R., XU, X.,
903 OCAMPO, A., YUAN, T., YANG, J., LI, Y., SHI, L., GUAN, D., PAN, H., DUAN,
904 S., DING, Z., LI, M., YI, F., BAI, R., WANG, Y., CHEN, C., YANG, F., LI, X.,
905 WANG, Z., AIZAWA, E., GOEBL, A., SOLIGALLA, R. D., REDDY, P., ESTEBAN,
906 C. R., TANG, F., LIU, G. H. & BELMONTE, J. C. 2015. Aging stem cells. A
907 Werner syndrome stem cell model unveils heterochromatin alterations as a driver
908 of human aging. *Science,* 348**,** 1160-3.
909
910
911
912
913

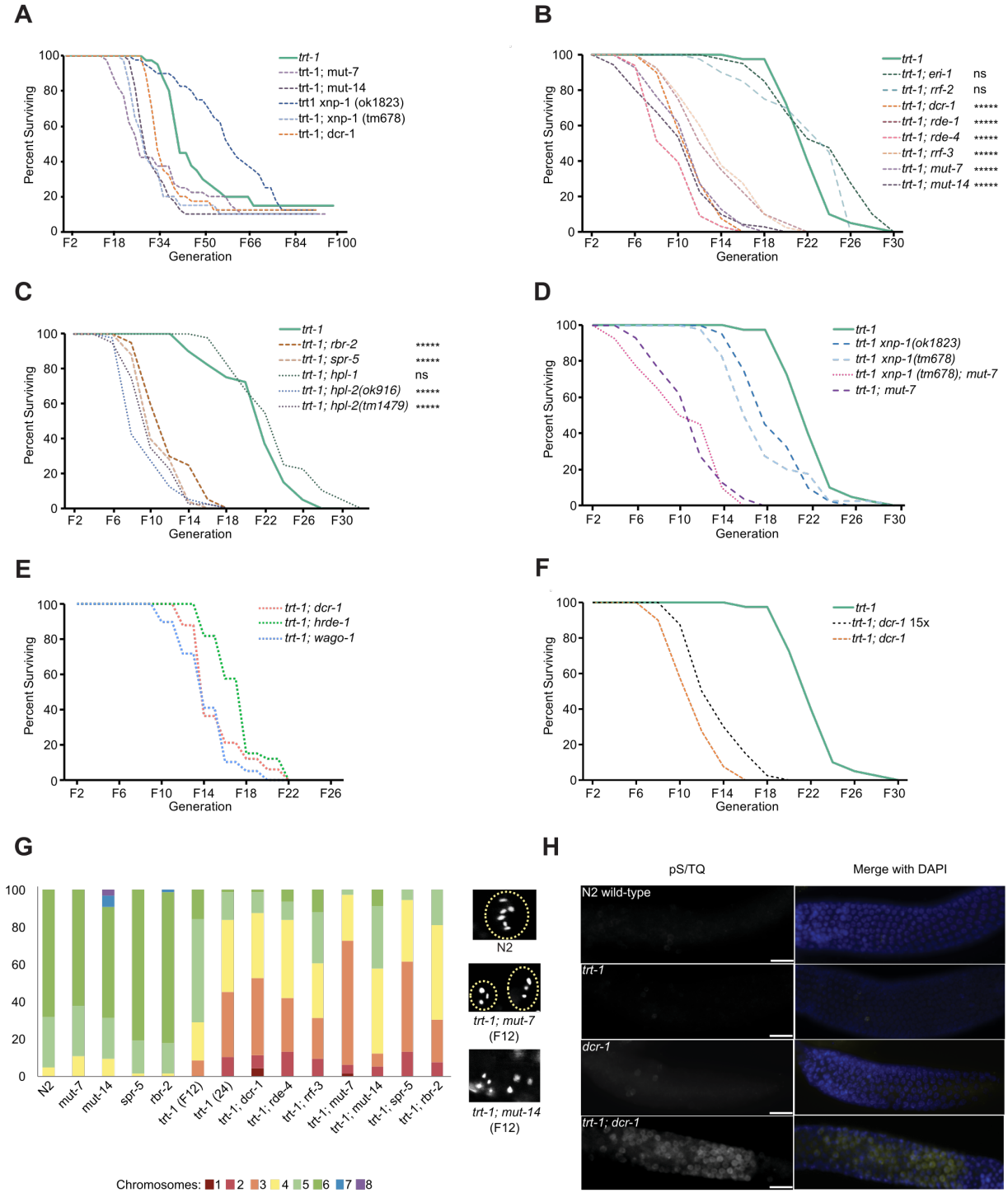

Figure 1: Endogenous small RNA and chromatin factors repress telomere stability in the absence of telomerase. (A) Survival curve of primary or secondary siRNA deficient telomerase mutants when 6 larval L1s are passaged weekly. (B) Survival curve of double mutants for *trt-1* and chromatin factors passaged by 6 L1s weekly. (C) Histone H3.3 remodeling protein XNP-1 represses senescence in *trt-1* mutants epistatically to the small RNA factor MUT-7. (D) Survival curve of telomerase-deficient strains

921 passaged at ~100 worms weekly for 40 independent lines. One allele of *xnp-1* (ok1823)
922 extended survival but did not increase survival via ALT (Table S1). (E) Small RNA and
923 heterochromatin mutant *trt-1* lines have high levels of chromosome fusions, comparable
924 to *tr-1* single mutants at F24. Fusions were assayed by diamidino-2-phenylindole (DAPI)
925 staining of oocytes in diakinesis. (F) High levels of phospho-(Ser/Thr) staining in the
926 meiotic gonad of *trt-1; dcr-1* at F6 compared to N2 or *trt-1*. Scale bar, 25□m. (B)-(D)
927 ***p < 0.001; ****p < 0.00001; ns, not significant, (Log rank test, n □□40 independent
928 lines for each genotype).
929

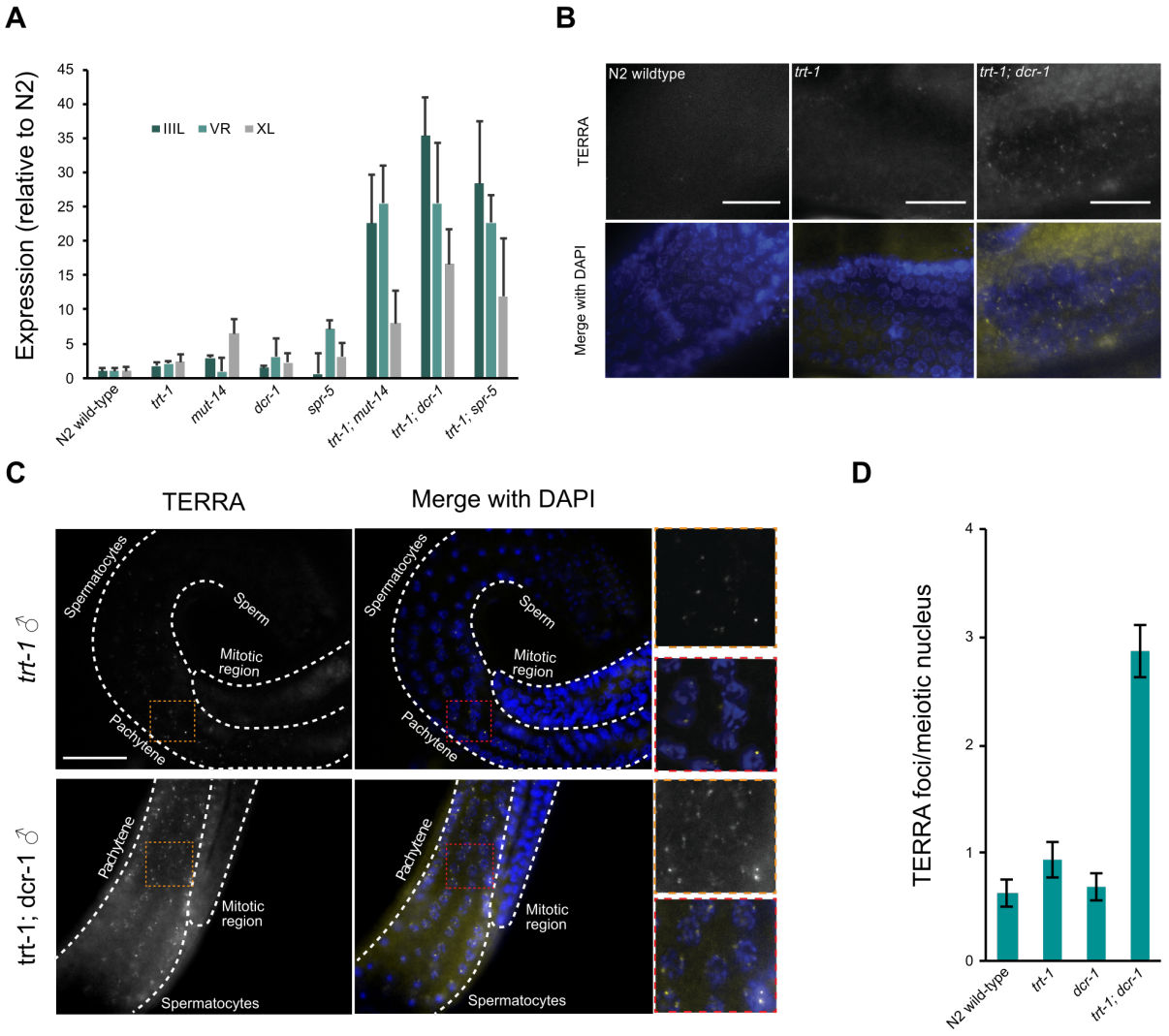

Figure 2: (A) Expression of TERRA from subtelomeres IIIL, VR, and XL is increased in siRNA and heterochromatin deficient telomerase mutants. cDNA was reverse transcribed with a telomere specific primer and qPCR was performed using subtelomere-specific primer pairs and normalized to *act-1*. Expression data are plotted relative to wildtype and represent the mean ± SEM of three biological replicates. (B) RNA FISH signals of TERRA in meiotic germlines of hermaphrodites of the indicated genotypes. TERRA foci are present in wildtype and *trt-1* in the pachytene region and increased in *trt-1; dcr-1.* Scale bar, 10um. (C) Representative RNA FISH images of TERRA in males show foci in the pachytene region of the germline which are increased in *trt-1; dcr-1* compared to *trt-1.* Scale bar, 20 um. (D) Quantification of germline TERRA foci (mean ± SEM, N=10 germlines).

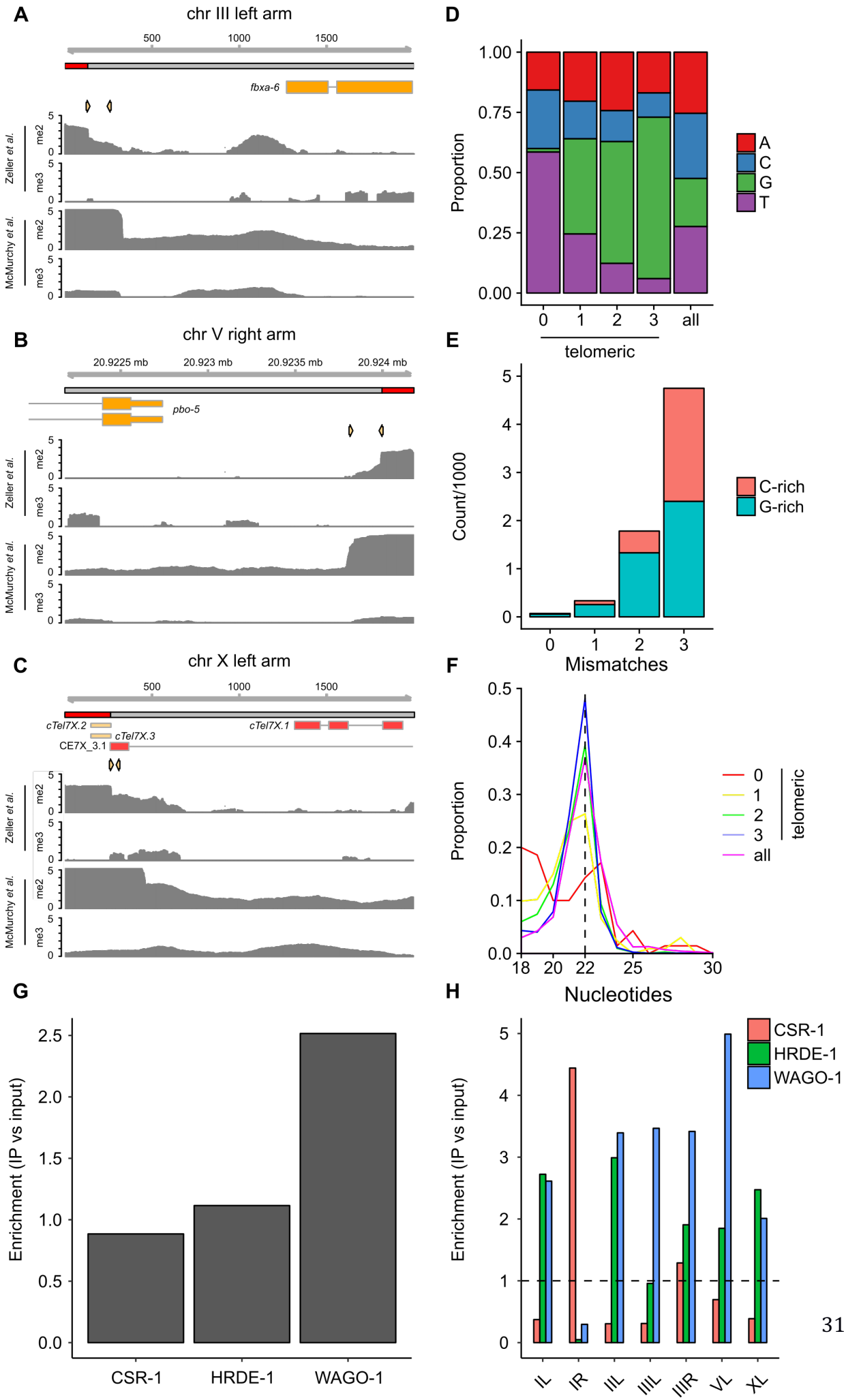
A
chr III left arm
500
1000
1500
fbxa-6
Zeller et al.
me2
me3
McMurchy et al.
B
chr V right arm
20.9225 mb
20.923 mb
20.9235 mb
20.924 mb
pbo-5
C
chr X left arm
cTel7X.2
cTel7X.3
CE7X_3.1
cTel7X.1
D
Proportion
A
C
G
T
0
1
2
3
all
telomeric
E
Count/1000
C-rich
G-rich
Mismatches
F
Proportion
Nucleotides
telomeric
G
Enrichment (IP vs input)
CSR-1
HRDE-1
WAGO-1
H
Enrichment (IP vs input)
CSR-1
HRDE-1
WAGO-1
IL
IR
IIL
IIIL
IIIR
VL
XL

944

945
946 **Figure 3:** Analysis of telomere-mapping small RNAs in published datasets. (A)-(C)
947 ChIP-seq enrichment profiles at three chromosome ends constructed using published
948 data (McMurchy et al., 2017, Zeller et al., 2016). Small orange arrows between gene
949 models and data tracks show the position of primers used in TERRA qRT-PCR
950 experiments. (D) Proportion of telomere-mapping small RNA reads in published data
951 beginning with a particular nucleotide. (E) Number of reads in published data mapping
952 to the G-rich (TTAGGC) or C-rich (GCCTAA) telomeric strand. (F) Distribution of small
953 RNA length in published data. (G) Enrichment (IP/input) of reads mapping to perfect
954 telomere sequence with up to three mismatches in published immunoprecipitation
955 datasets for three different Argonaute proteins. (H) Enrichment for subtelomeric siRNAs
956 for datasets used in (G). Numbers 0-3 in (D), (E) and (F) indicate number of
957 mismatches with perfect telomere.
958

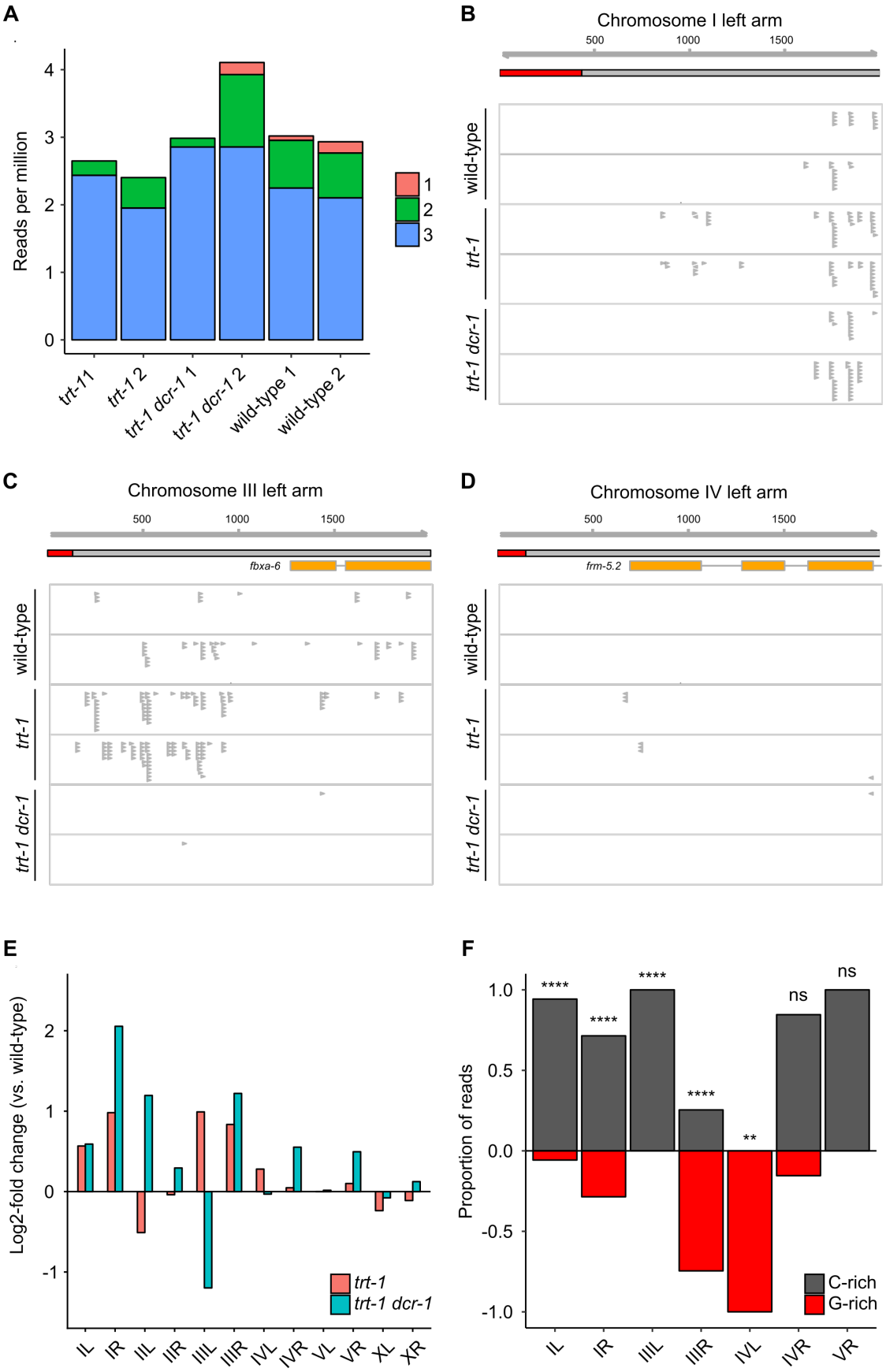
A
Reads per million
0
1
2
3
4
trt-1 1
trt-1 2
trt-1 dcr-1 1
trt-1 dcr-1 2
wild-type 1
wild-type 2
1
2
3
B
Chromosome I left arm
500
1000
1500
wild-type
trt-1
trt-1 dcr-1
C
Chromosome III left arm
500
1000
1500
fbxa-6
wild-type
trt-1
trt-1 dcr-1
D
Chromosome IV left arm
500
1000
1500
frm-5.2
wild-type
trt-1
trt-1 dcr-1
E
Log2-fold change (vs. wild-type)
-1
0
1
2
trt-1
trt-1 dcr-1
IL
IR
IIL
IIR
IIIL
IIIR
IVL
IVR
VL
VR
XL
XR
F
Proportion of reads
1.0
0.5
0.0
-0.5
-1.0
****
****
****
****
**
ns
ns
C-rich
G-rich
IL
IR
IIIL
IIIR
IVL
IVR
VR

959

960
961 **Figure 4:** Upregulation of subtelomeric siRNAs in telomerase mutants. (A) Number of
962 telomere-mapping reads in wild-type, trt-1 and trt-1;dcr-1 libraries. Numbers 1-3 indicate
963 number of mismatches. (B)-(D) 22G siRNAs at three subtelomeres. (E) Log2-fold
964 change in siRNA abundance at subtelomeres relative to wild-typein *trt-1* and *trt-1 dcr-1*
965 animals. (F) Proportion of subtelomeric siRNAs mapping to the strand corresponding to
966 the G-rich (TTAGGC) and C-rich (TAAGCC) telomere strand in *trt-1* animals. **** $p < 0.0001$; ** $p < 0.01$; ns, not significnat (Binomial test with Bonferroni correction).
968

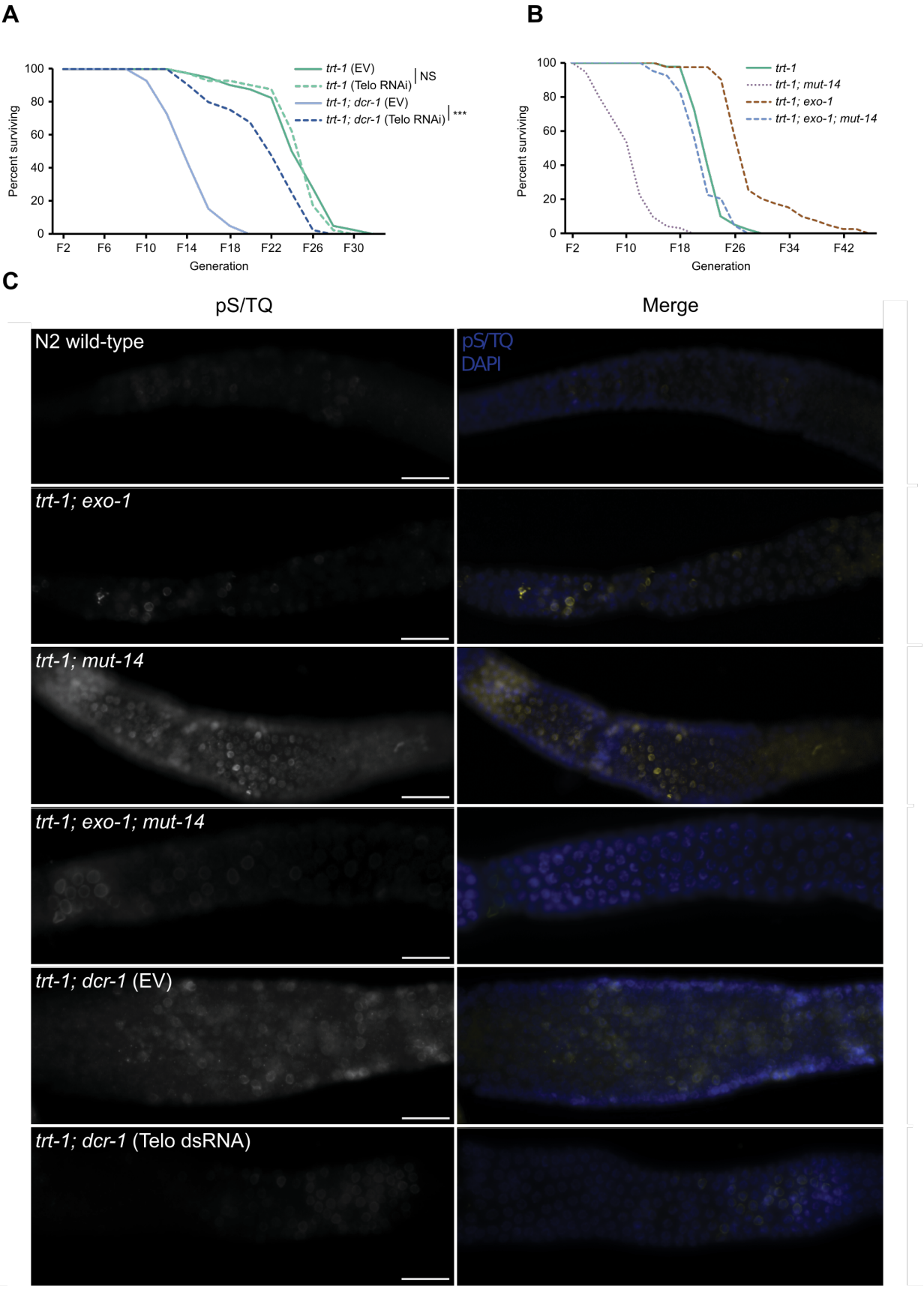
A
Percent surviving
100
80
60
40
20
0
F2
F6
F10
F14
F18
F22
F26
F30
Generation
trt-1 (EV)
trt-1 (Telo RNAi)
NS
trt-1; dcr-1 (EV)
trt-1; dcr-1 (Telo RNAi)
***
B
Percent surviving
100
80
60
40
20
0
F2
F10
F18
F26
F34
F42
Generation
trt-1
trt-1; mut-14
trt-1; exo-1
trt-1; exo-1; mut-14
C
pS/TQ
Merge
N2 wild-type
pS/TQ
DAPI
trt-1; exo-1
trt-1; mut-14
trt-1; exo-1; mut-14
trt-1; dcr-1 (EV)
trt-1; dcr-1 (Telo dsRNA)

969

970
971 **Figure 5** Fast senescence in siRNA-deficient *trt-1* is rescued by exogenous telomeric
972 dsRNA or loss of Exonuclease-1. (A) Survival of *trt-1* or *trt-1; dcr-1(mg375)* on either
973 empty vector control (EV) or bacteria expressing telomeric double-stranded RNA (telo
974 dsRNA). Log rank test relative to EV, ***P < 0.001 (B) Loss of exo-1 extends survival of
975 *trt-1; mut-14* lines. (C) Telomeric dsRNA and loss of exo-1 suppress accumulation of
976 phospho-(Ser/Thr) in siRNA-deficient *trt-1* by F6. Scale bar, 20um.
977
978
979
980

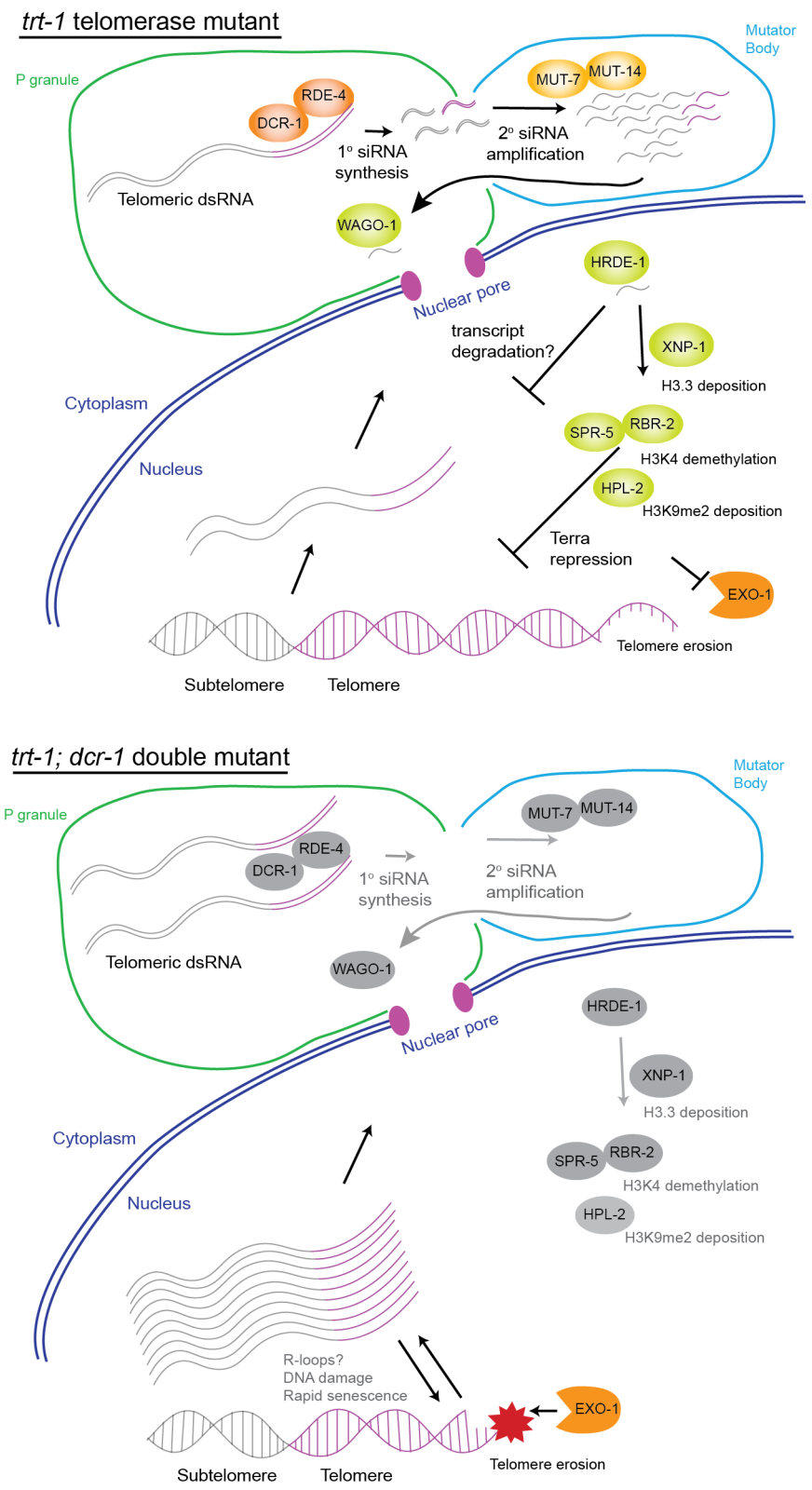

Figure 6: Model. In *trt-1* telomerase mutants, telomeric erosion induces expression of the lncRNA TERRA, which engages production of sub-telomeric and telomeric siRNAs.

Small RNAs promote deposition of H3K9me2 and H3K4 demethylation to maintain heterochromatic silencing of the telomere, repressing excess transcription, R-loop formation, DNA damage, and rapid senescence. In *trt-1; dcr-1* double mutants, TERRA expression is not repressed, leading to DNA damage, possibly RNA:DNA hybrids, and rapid senescence, which is dependent on the nuclease EXO-1.

Supplemental Information

5 Supplemental Figures

3 Supplemental Tables

1 Supplemental File

S1

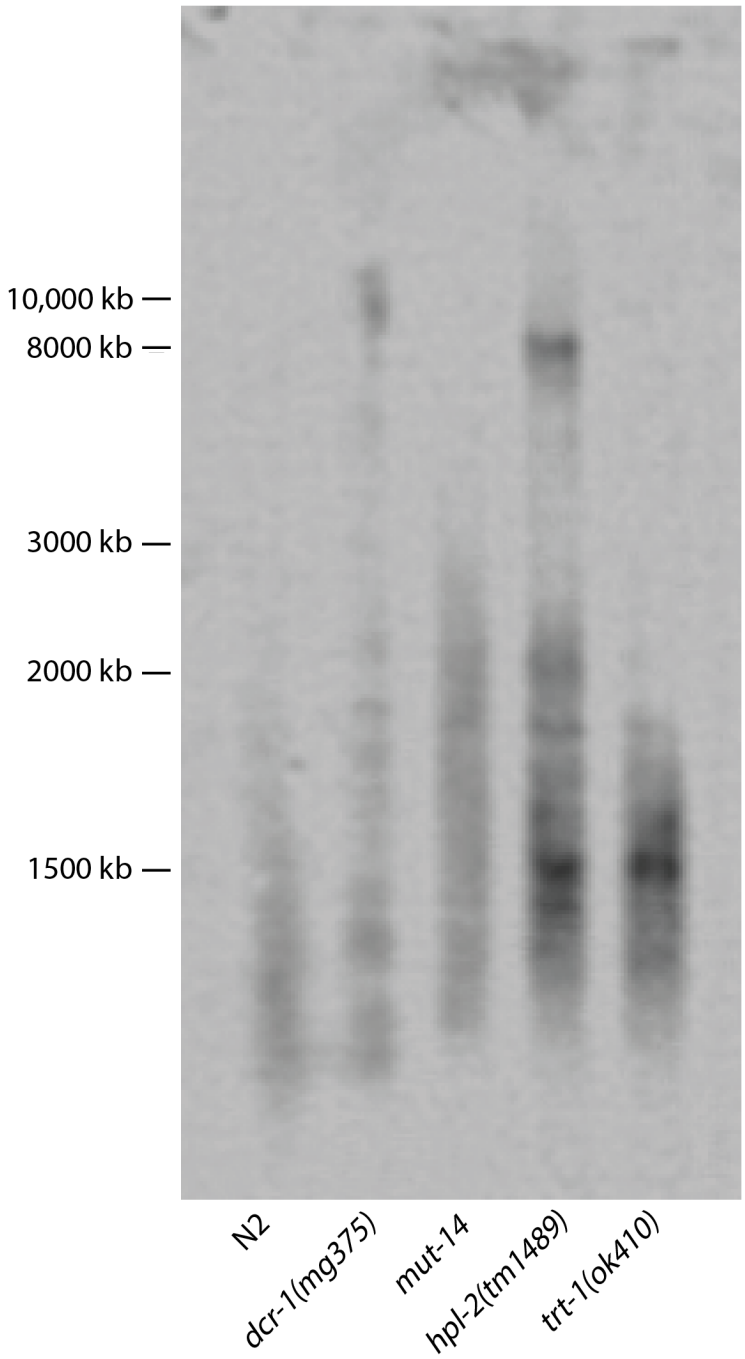

1007 **Figure S1. Related to Figure 1.** Terminal Restriction Fragment (TFR) analysis of
1008 wildtype and single mutant strains using a telomeric probe.

1009
1010
1011
1012
1013

S2

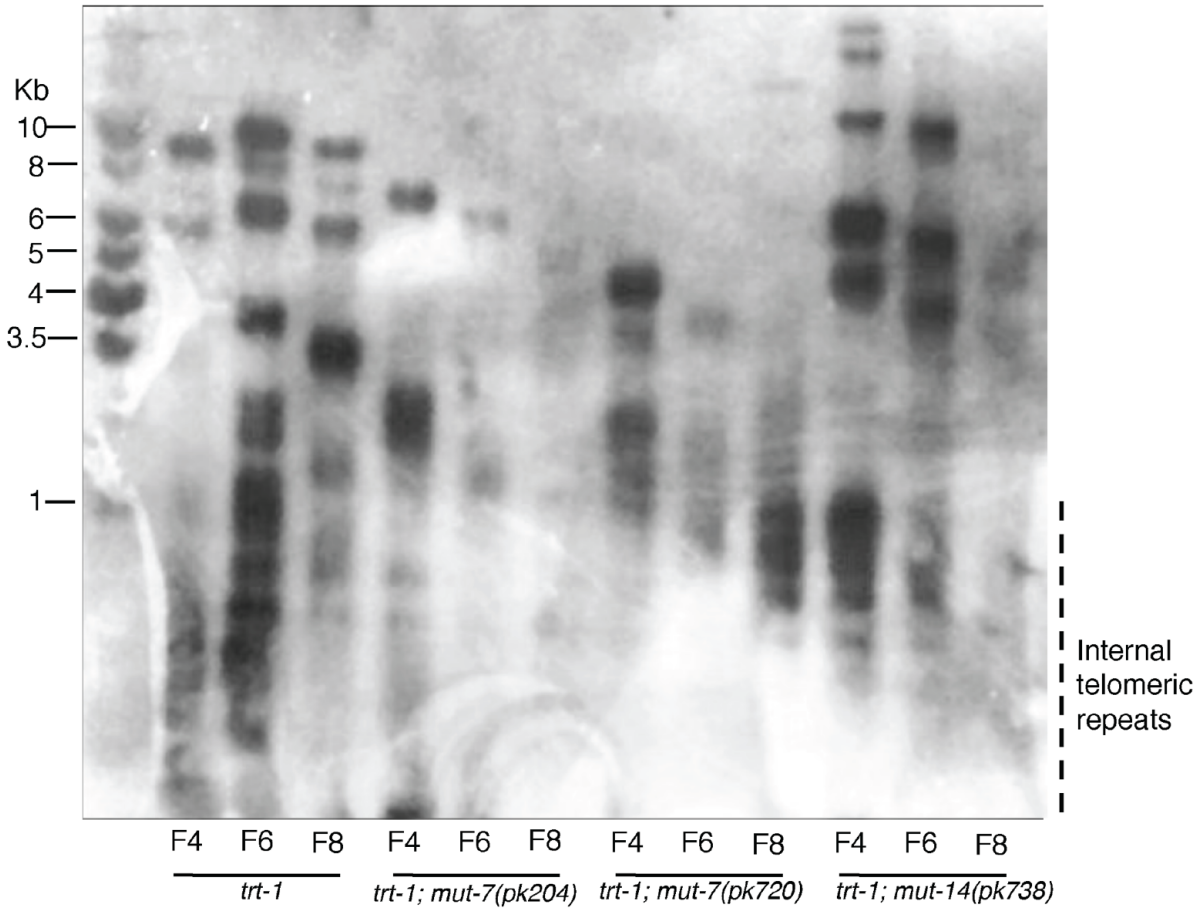

1014
1015
1016

1017 **Figure S2. Related to Figure 1.** TRF analysis of RNAi-deficient telomerase mutant
1018 strains using telomeric probe.

1019
1020

1021

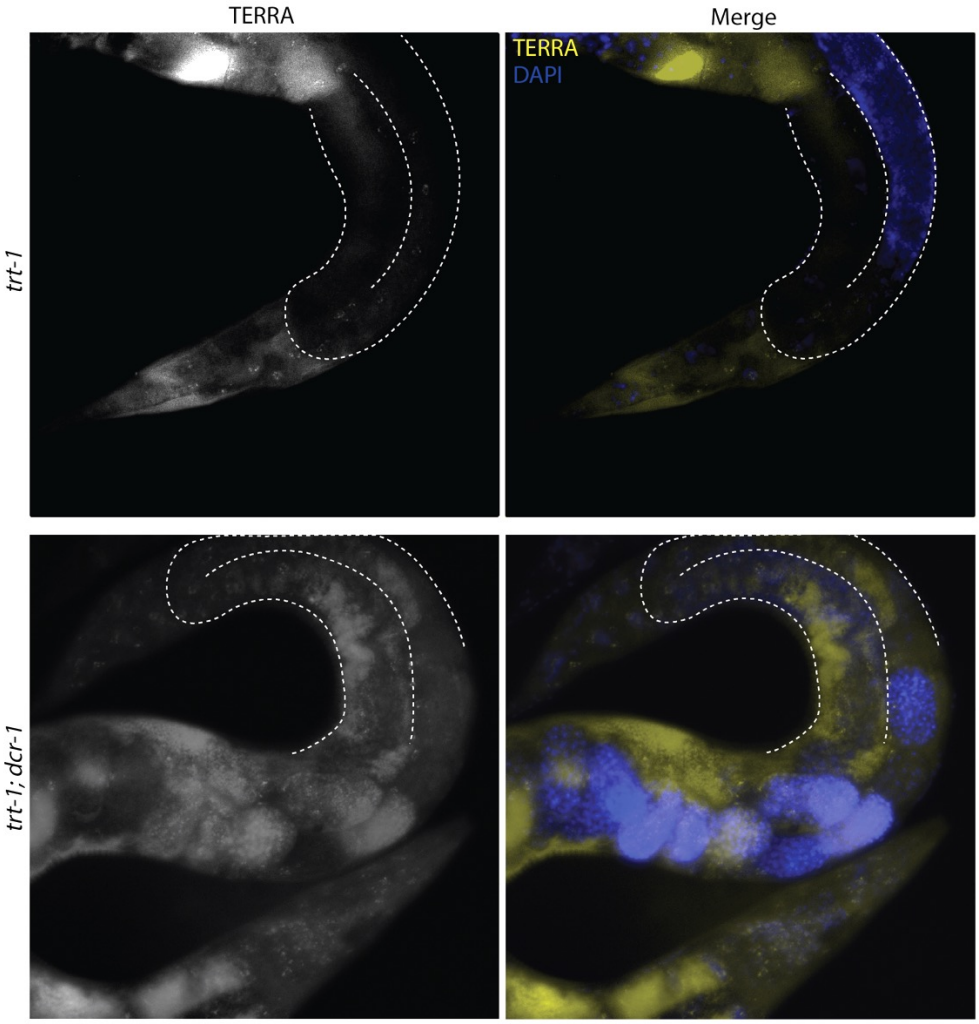

1022
1023
1024
1025

1026 **Figure S3. Related to Figure 2.** TERRA expression (yellow) in *trt-1* and *trt-1; dcr-*
1027 *1(mg375)* 1 day old adults detected with a Cy5-labelled telomeric probe.

1028
1029
1030
1031
1032
1033
1034
1035
1036

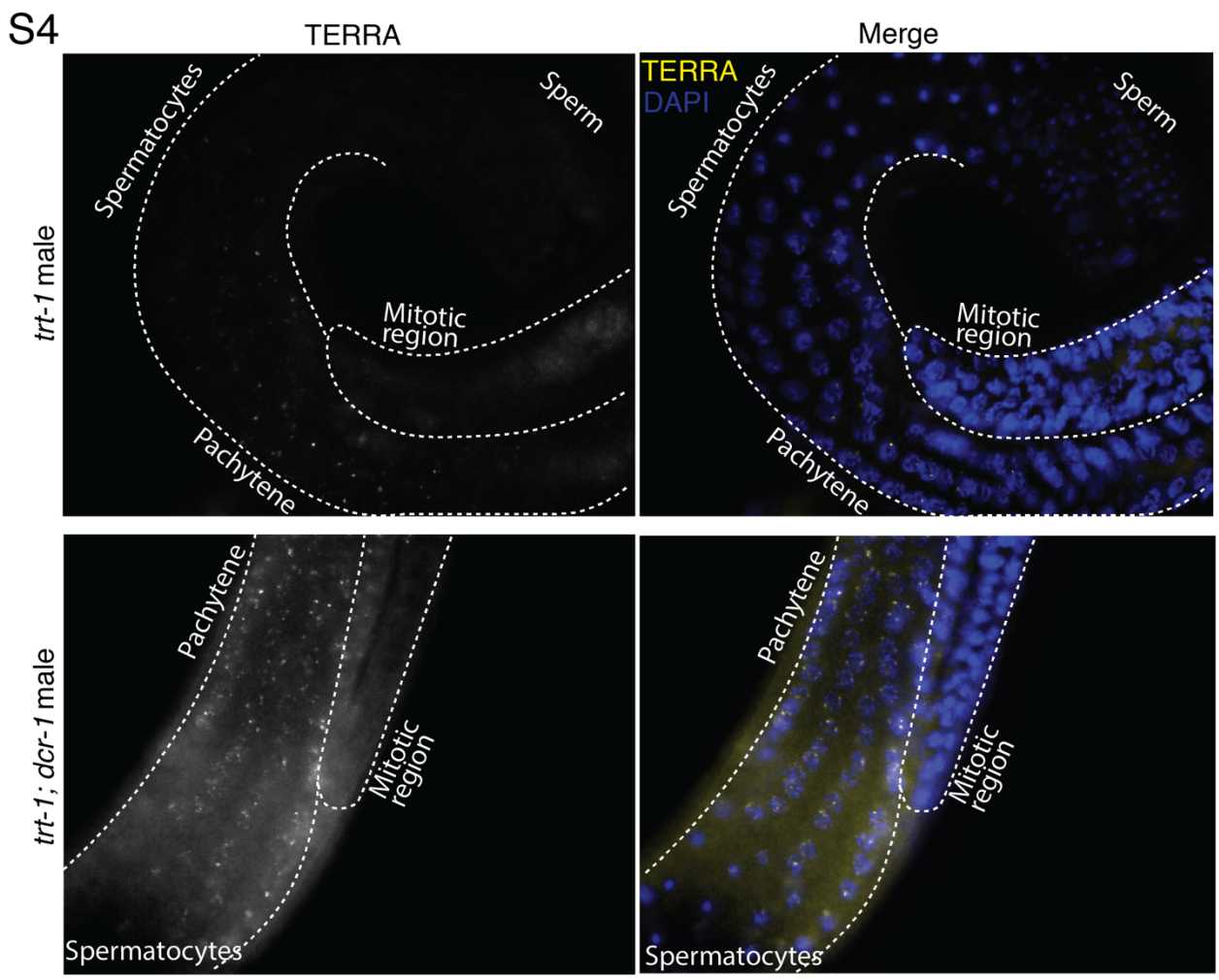

Figure S4. Related to Figure 2. RNA FISH of TERRA expression in *trt-1* and *trt-1; dcr-1* males. Note TERRA foci in the Pachytene region in both *trt-1* and *trt-1; dcr-1*, as well as lack of expression in the mitotic region and spermatocytes

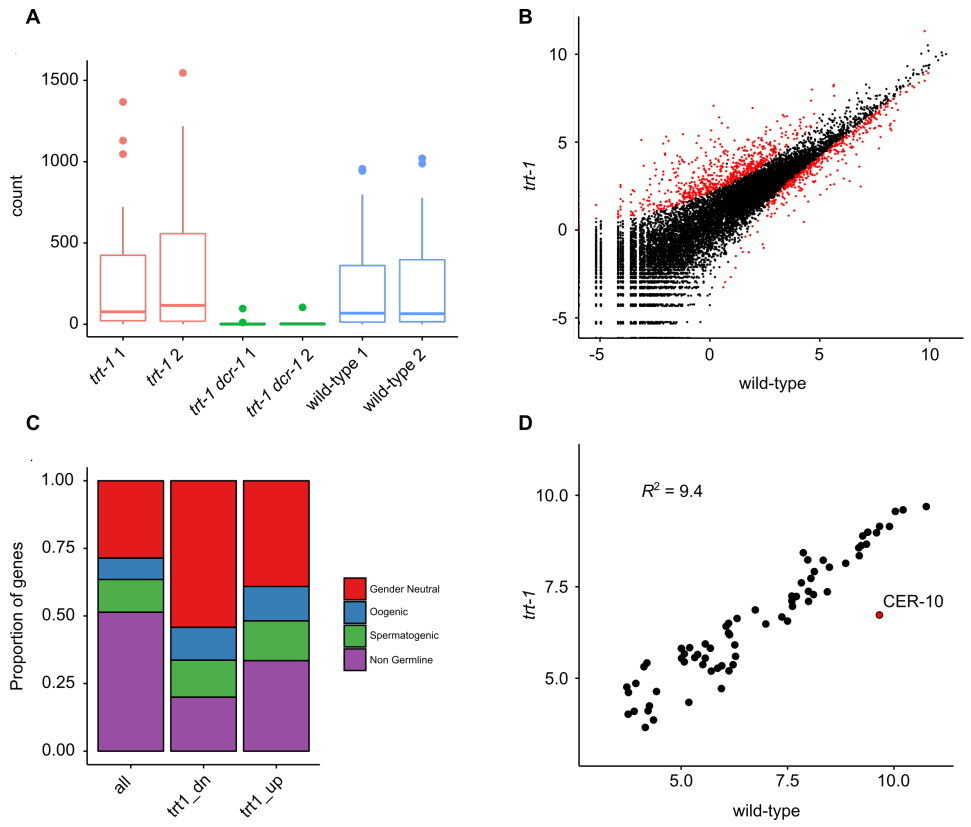

Figure S5. Related to Figure 3. Analysis of 22G small RNA species in telomerase and Dicer mutants. (A) Number of reads mapping to DCR-1 targets identified by Gent *et al.* (Gent et al., 2010). (B) log2 normalized mean read counts at every *C. elegans* gene for *trt-1* and wild-type. Genes identified as significantly differentially expressed by DESeq2 are shown in red. (C) Proportion of all genes or genes downregulated (trt1_dn) or upregulated (trt1_up) belonging to expression categories defined by Ortiz *et al.* (see reference 54 in main text). (D) log2 normalized mean read counts at transposon consensus sequences for *trt-1* and wild-type.

	Lines tested	Number ALT Survivors	Z score	p-value (two tailed)
trt-1	40	6		
trt-1; mut-7(pk204)	40	4	0.6761	0.4965
trt-1; mut-14(pk738)	40	4	0.6761	0.4965
trt-1 xnp-1(ok1823)	40	6	0	1
trt-1 xnp-1(tm678)	40	4	0.6761	0.4965
trt-1; dcr-1 (mg375)	40	5	0.3247	0.74896

Supplemental Table S1. Related to Figure 1. Statistical analysis of ALT survival strains. Loss of endogenous siRNA production (*mut-7*, *mut-14*, and *dcr-1*) or histone chaperone XNP-1/ATRX does not increase survival via ALT.

Strain	Log Rank test (Z=)	p-value
trt-1; mut-7(pk204)	9.79	<0.00001
trt-1; mut-14(pk738)	9.96	<0.00001
trt-1; dcr-1(mg375)	9.37	<0.00001
trt-1; rde-1	8.23	<0.00001
trt-1; rde-4	9.21	<0.00001
trt-1; rrf-3	8.4	<0.00001
trt-1; rrf-2	1.7	0.089
trt-1; exo-1	7.38	<0.00001
trt-1 xnp-1(ok1823)	4.3	<0.00001
trt-1 xnp-1(tm678)	4.23	<0.0001
trt-1 xnp-1(tm678); mut-7	9.21	<0.00001
trt-1; sid-1	6.52	<0.00001
trt-1; rbr-2(tm1231)	8.64	<0.00001
trt-1; spr-5 (by101)	8.89	<0.00001

Supplemental Table S2. Related to Figure 1. Log rank analysis of survival curves. N=40 independent lines for each genotype. Strains were passaged by transferring 6 larval L1s weekly and scored as sterile when plates contained no new L1 larvae.

1148
1149

trt-1 F1	males	dead embryos	*trt-1; dcr-1* F1	males	dead embryos
A1	13	6	A1	0	0
A2	4	26	A2	0	0
A3	8	24	A3	1	0
D1	10	11	A4	0	0
D2	11	4	B1	0	0
D3	4	9	B2	0	0
D4	13	15	B3	0	0
			B4	0	0
			C1	0	0
			C2	0	6
			C3	1	0
			C4	0	0
			D1	0	0
			D2	0	0
			D3	0	0
			D4	0	0

1150
1151
1152
1153 **Supplemental Table S3. Related to Figure 1.** Counts of total F2 males and dead
1154 embryos scored for F1 progeny from crosses of wildtype males with either late-
1155 generation F16 *trt-1* mutant controls (n=2 independently grown strains, three F1 scored
1156 for strain A and four for strain D) or early generation F4 *trt-1; dcr-1* double mutant (n=4
1157 strains, 4 F1 each scored for strains A, B, C and D) hermaphrodites. If a chromosome
1158 fusion is present in any of the F1 animals, then it will cause weak non-disjunction of the
1159 fused chromosomes, which leads to F2 dead embryos if an autosome is fused or to F2
1160 males if the X chromosome is fused.
1161
1162
1163 **Supplemental File 1. Related to Figure 3.** Levels of telomeric siRNAs from wild-type
1164 and those of small RNA mutants.
1165